JCI The Journal of Clinical Investigation

Imaging neuroinflammation in individuals with substance use disorders

Xinyi Li, … , Nora D. Volkow, Corinde E. Wiers

J Clin Invest. 2024;134(11):e172884. https://doi.org/10.1172/JCI172884.

Review Series

Increasing evidence suggests a role of neuroinflammation in substance use disorders (SUDs). This Review presents findings from neuroimaging studies assessing brain markers of inflammation in vivo in individuals with SUDs. Most studies investigated the translocator protein 18 kDa (TSPO) using PET; neuroimmune markers myo-inositol, choline-containing compounds, and N-acetyl aspartate using magnetic resonance spectroscopy; and fractional anisotropy using MRI. Study findings have contributed to a greater understanding of neuroimmune function in the pathophysiology of SUDs, including its temporal dynamics (i.e., acute versus chronic substance use) and new targets for SUD treatment.

Imaging neuroinflammation in individuals with substance use disorders

Xinyi Li,[1] Astrid P. Ramos-Rolón,[1] Gabriel Kass,[1] Lais S. Pereira-Rufino,[2] Naomi Shifman,[1] Zhenhao Shi,[1] Nora D. Volkow,[3] and Corinde E. Wiers[1]

[1]Center for Studies of Addiction, University of Pennsylvania Perelman School of Medicine, Department of Psychiatry, Philadelphia, Pennsylvania, USA. [2]Departamento de Morfologia e Genética, Escola Paulista de Medicina, Universidade Federal de São Paulo, São Paulo, Brazil. [3]Laboratory of Neuroimaging, National Institute on Alcohol Abuse and Alcoholism, NIH, Bethesda, Maryland, USA.

Increasing evidence suggests a role of neuroinflammation in substance use disorders (SUDs). This Review presents findings from neuroimaging studies assessing brain markers of inflammation in vivo in individuals with SUDs. Most studies investigated the translocator protein 18 kDa (TSPO) using PET; neuroimmune markers myo-inositol, choline-containing compounds, and N-acetyl aspartate using magnetic resonance spectroscopy; and fractional anisotropy using MRI. Study findings have contributed to a greater understanding of neuroimmune function in the pathophysiology of SUDs, including its temporal dynamics (i.e., acute versus chronic substance use) and new targets for SUD treatment.

Introduction

Substance use disorders (SUD) cause substantial economic and public health challenges globally. In the United States, over 46.3 million Americans aged 12 years or older were affected by SUDs in 2021. SUDs are chronic relapsing multifactorial disorders characterized by a range of structural and functional changes in the brain, as revealed by preclinical and human neuroimaging studies (1). The heuristic framework for SUD outlines a three-stage recurring cycle of binge/intoxication, withdrawal/negative affect, and preoccupation/anticipation that is governed by three functional domains (incentive salience, negative emotional states, and executive functions) (2). Engagement of the mesocorticolimbic system, consisting of the ventral tegmental area (VTA), striatum, prefrontal cortex, amygdala, and hippocampus, in the binge/intoxication stage heightens the incentive saliency of misused drugs, forms conditioned responses to drug-related cues, and facilitates maladaptive habit formation/compulsive drug behaviors (2). Discontinuing substance use produces symptoms of withdrawal and negative effects, which are mediated by brain regions involved in stress response and emotional regulation (i.e., the amygdala) (2). Reconciling memories of previous drug use (amygdala and hippocampus), craving (prefrontal cortex and striatum), and decreasing executive control (prefrontal cortex) in the preoccupation/anticipation stage subsequently leads to relapse and perpetuates SUD (3). These functional and structural neuroadaptations may be attributable to neuroinflammation following prolonged substance use that increases neurotoxicity and promotes neurodegeneration in individuals with SUD (4).

Inflammation is a biological process triggered by a variety of harmful insults, such as infection, ischemia, stress, and trauma (5, 6). In the CNS, a key element of neuroinflammation is the activation of immune-specific cells (i.e., microglia and astrocytes) that synthesize inflammatory mediators and promote leukocyte recruitment. Activation of the TLRs on microglia by pathogen-associated or internal damage-associated molecular patterns initiates the immune response. The activated TLRs promote the recruitment of NF-κB, resulting in the production of different mediators, such as proinflammatory cytokines (e.g., IL-6, IL-1, and TNF-α), type I interferon (IFN-β), chemokines (CCL5), and cyclooxygenase-2 (COX-2) (7, 8).

Studies on postmortem markers of inflammation revealed increased markers of microglia in the cingulate cortex, VTA, amygdala, and midbrain of individuals with alcohol use disorder (AUD) compared with those of nondependent controls (9, 10). They also showed higher expression of TLRs and downstream signaling cascade NF-κB in the orbital frontal cortex and higher concentration of proinflammatory cytokines (i.e., monocyte chemoattractant protein-1) in the VTA, hippocampus, and amygdala (10–12). Similarly, chronic opioid exposure has been associated with upregulation of glial activation and immune response pathways (13). While the initial stage of neuroinflammation may be beneficial and protective, overactivation of TLRs in prolonged inflammation promotes cytotoxic changes, including the development of brain edema, gliosis, blood-brain barrier disruption, astrocyte proliferation, oxidative stress, and changes in cell survival transcription factors (14). Neuroinflammation was associated with neurodegeneration in neuropsychiatric disorders (7, 15) and may mediate structural and functional deficits that contribute to SUD.

The present Review focuses on the link between SUD and neuroinflammation based on human neuroimaging studies using PET and MRI (Figure 1). We will discuss findings that pertain to common substances of misuse, including alcohol, nicotine, opioids, cannabis, and stimulants.

Authorship note: XL and APRR contributed equally to this work.
Conflict of interest: The authors have declared that no conflict of interest exists.

Reference information: *J Clin Invest*. 2024;134(11):e172884.
https://doi.org/10.1172/JCI172884.

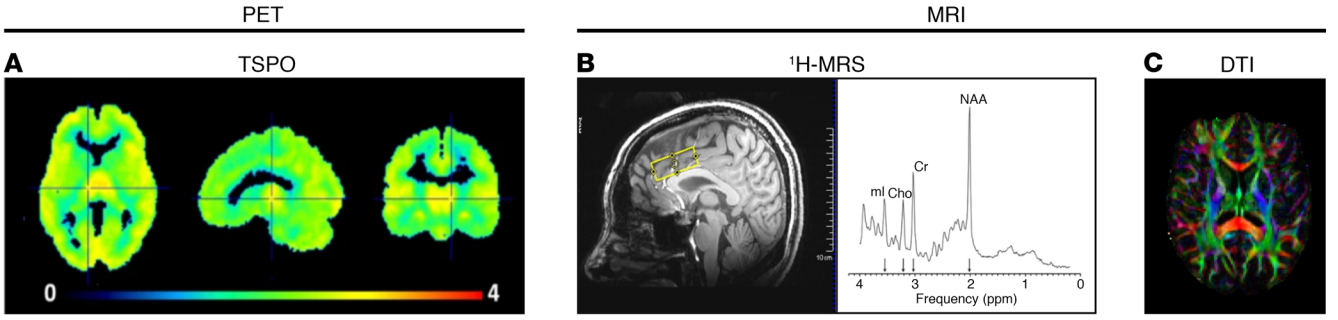

Figure 1. Imaging markers of neuroinflammation. (**A**) PET image of TSPO radiotracer [^{11}C]PBR28 (image reproduced with permission from Kim et al., 2018, ref. 21). (**B**) Representative image of ^{1}H-MRS voxel placement in the dorsal anterior cingulate cortex and ^{1}H-MRS spectra of inflammation markers, NAA, cho, and mI (spectra image reproduced with permission from Blüml, 2013, ref. 130). (**C**) DTI fractional anisotropy (FA) color map. Cho, choline-containing compounds; Cr, creatine; DTI, diffusion tensor imaging; ^{1}H-MRS, magnetic resonance spectroscopy; mI, myo-inositol; NAA, N-acetyl-aspartate; TSPO, translocator protein 18 kDa.

PET imaging: TSPO

Studies using PET to examine neuroinflammation have mainly focused on measures of translocator protein 18 kDa (TSPO) expression and binding. TSPO is a transmembrane protein localized in the outer mitochondrial membrane that mediates essential mitochondrial functions, such as regulating cholesterol transport steroid hormone synthesis, apoptosis, and cell proliferation (16). Within the CNS, TSPO is primarily expressed in microglia and reactive astrocytes, which are immune cells integral to the brain, and serves as a marker for immune system activation (4, 17). Several PET radiotracers have been developed to detect TSPO, including [^{11}C]PK11195, [^{11}C]PBR28, [^{11}C]DAA1106, and [^{18}F]FEPPA (4, 17). A summary of studies measuring TSPO in participants with SUD compared with nondependent controls is provided in Table 1.

Alcohol. Thus far, three studies have compared TSPO binding in AUD, and all found, contrary to their hypothesis, lower [^{11}C]PBR28 volumes of distribution (V_T) in individuals with AUD compared with that in healthy, nondependent control groups (meta-analyzed in ref. 18). Kalk et al. were the first to report lower hippocampal [^{11}C]PBR28 V_T in individuals with AUD compared with individuals acting as controls and nonsignificant trends for lower [^{11}C]PBR28 V_T in the midbrain, thalamus, cerebellum, and anterior cingulate cortex (ACC) (19). However, the recruited individuals with AUD were more likely to be smokers (8 of 9) than the people in the control group (5 of 20), and differences in smoking status may had confounding effects on the study results. The findings are concordant with those of another study that reported lower [^{11}C]PBR28 V_T in individuals with AUD than in controls matched for smoking status. Post hoc analyses examining regional differences in [^{11}C]PBR28 V_T revealed a significant effect of AUD in the cerebellum and trends for the frontal cortex, striatum, and hippocampus. Additional exploratory analysis indicated that [^{11}C]PBR28 V_T negatively correlated with alcohol dependence severity and number of drinks per day in the past month (20). Kim et al. (21) found no significant group differences in whole-brain [^{11}C]PBR28 binding between individuals with AUD and controls, but when separated by TSPO genotype (medium vs. high-affinity binding), those with the medium-affinity genotype and AUD had lower [^{11}C]PBR28 V_T than controls in the whole brain, gray matter, white matter, hippocampus, and thalamus. Although the study did not match for smoking status (10 of 19 smokers in the AUD group and no smokers in the control group), additional analyses showed no effects of smoking status on TSPO binding within the AUD group.

Despite the directionally consistent findings, they should be interpreted with the following considerations. Laurell et al. (22) reanalyzed data collected by Hillmer et al. (20) and separated total V_T into ligand-specific distribution volume (V_S) and non-displaceable-binding distribution volume (V_{ND}). AUD compared with healthy controls demonstrated significantly lower V_{ND} but no differences in V_S (22), raising the possibility that differences in [^{11}C]PBR28 V_T between patients and controls may be attributable to non-displaceable- instead of ligand-specific binding. Second, participants' blood cholesterol and triglyceride levels correlated inversely with [^{11}C]PBR28 (21, 23), as cholesterol binds to TSPO for transport during steroid synthesis (24). Dyslipidemia is evidenced in AUD (25), and the lower [^{11}C]PBR28 binding reported by PET studies may reflect greater competition from cholesterol for binding to TSPO in AUD. Third, rs6971 TSPO genotype (high-affinity binders, low-affinity binders, and mixed-affinity binders) has been shown to alter the affinity of [^{11}C]PBR28 for TSPO (22) and lipid levels (25) and may have implications for influencing the relationship between TSPO and AUD status (21). Thus, more work is needed to conclusively identify the mechanisms underlying lower TSPO in AUD.

A study that evaluated the effects of an acute oral alcohol challenge (adjusted to achieve a blood alcohol level of 80 mg/dL) in healthy volunteers found that alcohol increased [^{11}C]PBR28 V_T by an average of 12% (26). Alcohol-induced increases in [^{11}C]PBR28 V_T correlated negatively with the subjective effects of alcohol (26). This is in line with findings from a previous study in baboons that also found higher [^{18}F]DPA-714 V_T (58%–138%) in animals exposed to an acute intravenous alcohol infusion of 0.7–1 g/L compared with alcohol-naive animals (27). Although TSPO levels were reduced 7–12 months after the alcohol infusion in the alcohol-exposed animals, levels remained higher than those in alcohol-naive animals. The mechanisms underlying the differential effects of acute versus chronic alcohol adminis-

Table 1. PET studies of TSPO levels in individuals with SUDs

Authors (yr) (ref.)	Study population	Substance studied	Length since last use	Tracer	Group differences
Kalk et al. (2017) (19)	9 AUD, 20 controls	Alcohol	<1 month of medically assisted withdrawal	[^{11}C]PBR28	↓
Hillmer et al. (2017) (20)	15 AUD, 15 controls	Alcohol	1–24 days	[^{11}C]PBR28	↓
Kim et al. (2018) (21)	19 AUD, 17 controls	Alcohol	0–7 days	[^{11}C]PBR28	↓[A]
Brody et al. (2017) (28)	30 smokers, 15 controls	Tobacco	Satiated	[^{11}C]DAA1106	↓
Brody et al. (2018) (29)	22 smokers, 18 controls	Tobacco	Overnight abstinence	[^{11}C]DAA1106	↓
Hillmer et al. (2020) (30)	20 smokers, 20 controls	Tobacco	2–14 hours	[^{11}C]PBR28	⟷
Narendran et al. (2014) (35)	15 CUD, 17 controls	Cocaine	14 days	[^{11}C]PBR28	⟷
Sekine et al. (2008) (32)	12 MA use, 12 controls	Methamphetamine	0.5–4 years	[^{11}C](R)-PK11195	↑
London et al. (2020) (33)	11 MA use, 12 controls	Methamphetamine	≥4 days to <6 months	[^{11}C]DAA1106	⟷
Rathitharan et al. (2021) (34)	11 MA use, 26 controls	Methamphetamine	14.3–110 hours	[^{18}F]FEPPA	⟷
Da Silva et al. (2019) (36)	24 cannabis users, 27 controls	Cannabis	≥12 hours	[^{18}F]FEPPA	↑

Arrows in the group differences column indicate whether there was higher tracer binding/uptake in the SUD population than in controls (↑), lower tracer binding/uptake in the SUD population than in controls (↓), or no difference between groups (⟷). [A]Only in individuals with medium-affinity binding TSPO genotypes. AUD, alcohol use disorder; CUD, cocaine use disorder; MA, methamphetamine.

tration on brain TSPO levels require further elucidation. It has been postulated that chronic microglial activation in response to chronic alcohol use diminishes TSPO levels and the subsequent reduced immune response in AUD contributes to an enhanced susceptibility to diseases (20). In line with this, individuals with AUD showed lower peripheral cytokine response to stimulation with LPS than controls (20).

Tobacco. One study in nicotine users showed 16.8% lower whole-brain [^{11}C]DAA1106 binding (measured as standard uptake values [SUVs]) in smokers during smoking satiety (i.e., having smoked ~15 minutes prior to scanning procedures) compared with nonsmokers on all volumes of interest (VOIs): amygdala, caudate, accumbens, hippocampus, putamen, and thalamus (28). A subsequent study showed that [^{11}C]DAA1106 SUVs in smokers remained low, even following overnight (~12 hours) abstinence in the same VOIs as the previous study (29). Higher levels of cigarette exposure, as indicated by the depth of inhalation (29) or cigarettes per day (28), were associated with lower [^{11}C]DAA1106 binding, which was interpreted as reduced TPSO levels. The type of cigarette also altered TSPO levels, as three-way comparisons showed that SUV was highest in nonsmokers, in the middle in nonmenthol cigarette smokers, and lowest in menthol cigarette smokers (28, 29). In contrast, another study found no significant differences in [^{11}C]PBR28 binding (measured as V_T) between smokers (abstinent for 2–14 hours before the scan) and nonsmokers in whole brain or any of the VOIs (30). The inconsistent study findings may be attributable to differences in radioligands ([^{11}C]PBR28 vs. [^{11}C]DAA1106) or quantification methods (SUV vs. V_T). V_T is the gold-standard quantification method that, unlike SUV, accounts for plasma radioligand concentration and potential differences in radioligand delivery to the brain (31). Yoder et al., retrospectively compared SUVs and V_T from [^{11}C]PBR28 PET scans acquired in baboons at baseline and at varying time points following LPS injections. Although regional SUV and V_T were highly correlated, the slope of their relationships varied across individuals and ROIs, suggesting discrepancies between SUV and V_T (31).

Stimulants. An early study using the TSPO tracer [^{11}C]*(R)*-PK11195 demonstrated higher binding (measured as binding potential) in individuals with a history of methamphetamine use disorder (MUD; abstinent 0.5–4 years) than healthy volunteers in the midbrain, striatum, thalamus, orbitofrontal cortex, and insular cortex (32). *(R)*-PK11195 binding potential was negatively correlated with the duration of abstinence in the midbrain, striatum, and thalamus, suggesting that dysregulation in neuronal immune response may normalize with prolonged abstinence (32). A later study by London et al., quantifying TSPO binding with SUV and newer generation of TSPO PET radiotracers, [^{11}C]DAA1106, found no differences between individuals with MUD in early abstinence (<6 months) and healthy controls in whole-brain TSPO levels or any of the examined VOIs (33). Similarly, Rathitharan et al. (34) measured [18C]FEPPA V_T and did not demonstrate significant group differences in TSPO binding. The inconsistent findings may be attributable to the high nonspecific binding of [^{11}C] *(R)*-PK11195 compared with the newer TSPO PET tracers, PET quantification methods, or study differences in participant characteristics (e.g., early vs. prolonged abstinence or MUD severity) and additional studies are warranted.

A study of cocaine use disorder (CUD) found no significant differences in [^{11}C]PBR28 V_T between recently abstinent cocaine-dependent individuals and nondependent controls in the midbrain, striatum, cerebral cortex, ACC, medial temporal lobe, or cerebellum (35).

Cannabis. In the only clinical study examining the effects of cannabis on TSPO, long-term cannabis users (use >4 times/week for the past 12 months) had higher brain [^{18}F]FEPPA V_T than controls in total and across the dorsolateral prefrontal cortex (dlPFC), medial prefrontal cortex, temporal cortex, ACC, cerebellum, and gray matter as a whole. More prominent effects were observed in a subset of individuals who met the diagnostic criteria for cannabis use disorder. Exploratory analysis in cannabis users demonstrated that [18F]FEPPA V_T negatively correlated with lifetime cannabis use, which remained trending but no longer significant after controlling for sex, but not cannabis craving and dependence severity (36).

Opioids. To the best of our knowledge, no human studies have been published on the effect of opioids on brain TSPO binding.

MRI: magnetic resonance spectroscopy

Proton magnetic resonance spectroscopy (^{1}H-MRS) is a noninvasive neuroimaging technique that uses the MRI scanner to measure local concentrations of neuroinflammatory biomarkers: (a) myo-inositol (mI), an organic molecule present in glial cells that serves as a marker for glial cell activation and neuroinflammation; (b) N-acetyl aspartate (NAA), a neuronal marker, decreasing levels of which are indicative of neuronal dysfunction; (c) choline-containing compounds (Cho), which reflect membrane turnover; and (d) glutathione (GSH), which is involved in the cellular defense against oxidative stress and provides information on cellular inflammatory processes. Levels of brain metabolites are commonly expressed relative to creatine (Cre) or water, but absolute measures are also reported (37, 38). A summary of ^{1}H-MRS studies that included these inflammatory markers in individuals with SUDs compared with nondependent controls is provided in Tables 2 and 3.

Alcohol. A meta-analysis of 43 ^{1}H-MRS studies in individuals with AUD showed lower levels of NAA and Cho but no differences in mI compared with nondependent healthy volunteers (39). Specifically, lower levels of NAA and Cho were recorded in the frontal cortex, cerebellum, hippocampus, and frontal and parietal white matter. Lower Cho was also observed in the temporal cortex and thalamus, and NAA in the ACC (39). The concentrations of brain metabolites in individuals with AUD depend upon several factors, including individual drinking habits and duration of abstinence. For example, in individuals with AUD, the number of heavy drinking days in the 14 days prior to the MRI scan was inversely associated with dorsal ACC NAA/water (40), and more recent drinking correlated with lower NAA and Cho levels in frontal and thalamic regions (41). Lower hippocampal NAA (42) and greater thalamic mI levels (43) were observed in recently detoxified individuals with AUD though these measures recovered with abstinence.

Acute alcohol administration (0.65 g/kg in female users and 0.75 g/kg in male users) in healthy volunteers decreased Cho and mI in the frontal cortex and cerebellum 1.5 hours after ingestion compared with baseline but rebounded by 12 hours (44). Another study in which alcohol was infused intravenously to a target breath alcohol concentration of 60 mg/dL showed a similar reduction in Cho in the occipital cortex within an hour of administration but, in contrast to the previous study, found a trend for increasing mI as well as a decrease in NAA (45). Measurement of brain metabolites in the descending limb of the blood alcohol curve, approximately 4–5 hours following alcohol administration, demonstrated significant elevation in Cho/Cre and glutathione/Cre (GSH/Cre) in the thalamus but no effects on mI/Cre or NAA/Cre (46). The inconsistent findings of these studies raises questions about the temporal (i.e., ascending vs. descending limb) and regional (i.e., differing brain regions) effects of alcohol on brain metabolites.

Tobacco. Findings in individuals who smoke tobacco showed lower levels or no group differences in NAA, Cho, and mI levels compared with healthy controls (47). Low NAA levels, in particular, have been associated with poorer decision-making and higher impulsivity in smokers (47). Studies examining the role of abstinence and smoking severity on neuroinflammatory markers have yielded mixed results. Some reported no differences in neural metabolites between nicotine-deprived (24–72 h) and satiated states (48–50) or between individuals who smoke daily (>5 cigarettes/day) and those who smoke intermittently (1–4 cigarettes on at least 1 day per week) (51). Another study showed a positive correlation between lifetime tobacco exposure (pack-years) and ACC Cho levels (52).

Cigarette smoking often occurs concomitantly with heavy alcohol consumption and may exacerbate impairments in neural functioning in individuals with AUD. In comparison with nonsmoking individuals with AUD, those who smoked tobacco demonstrated lower NAA and Cho levels (53). Brain metabolite levels normalized with abstinence from alcohol in nonsmoking individuals with AUD but remained significantly reduced at 1 month in those who smoked (54). Abstinence-associated changes in Cho and mI levels correlated with improvements in visuospatial memory (54). Therefore, reductions in brain metabolites in smoking individuals with AUD may adversely affect their neural recovery (54).

Stimulants. Studies in individuals with MUD generally demonstrated lower NAA levels in frontal regions, including the ACC, but results for Cho and mI have been inconclusive (Table 3). Low NAA/Cre and Cho/Cre levels in the dlPFC and ACC correlated with neurocognitive impairments in individuals with MUD (55, 56). Greater duration of methamphetamine use was associated with greater reductions in NAA and mI (57). Prolonged abstinence may normalize brain metabolite levels. Thus, short-term abstinence from methamphetamine (1–6 months) resulted in lower NAA/Cre and higher mI/Cre compared with controls, but no differences were observed during longer-term abstinence (1–5 years) (58). Furthermore, the duration of abstinence was positively correlated with ACC NAA/Cre levels (58). Recovery may be slow, as one study demonstrated a persistent reduction in dlPFC NAA/Cre in individuals following approximately 5 weeks of abstinence (57).

An acute intravenous dose of cocaine (0.2 and 0.4 mg/kg) in occasional cocaine users increased NAA and Cho levels as compared with intravenous placebo (59). However, a comparison of individuals with CUD and healthy controls yielded no differences in ^{1}H-MRS makers of neuroinflammation (Table 3).

Cannabis. Administration of cannabis (300 μg/kg of Δ-9-tetrahydrocannabinol [THC]) versus placebo to occasional and heavy cannabis users increased mI/Cre in the striatum and ACC and NAA/Cre in the ACC, but only in the occasional users and not in the heavy users, suggesting cannabis tolerance in the latter group (60). Studies comparing cannabis users and controls generally indicated a decrease in mI (except for Muetzel et al., ref. 61, who found higher mI in female users compared with female nonusers but no differences between male users and nonusers) and no group differences in NAA and Cho levels (Table 3). Low mI levels significantly correlated with higher problematic drug use behavior and cannabis dependence (62), but no significant correlations were observed between brain metabolite levels and marijuana exposure (i.e., age of onset and total lifetime use) (63, 64). Cannabis-associated changes in brain metabolites may adversely affect neuropsychological performance. As such, thalamic mI/Cre levels were associated with greater cognitive impulsivity (64).

Opioids. Most ^{1}H-MRS studies in individuals with opioid use disorder (OUD) demonstrated low brain levels of NAA (Table 3). Methadone-treated individuals with OUD showed lower mI in the ACC than those maintained on buprenorphine, and the dose of methadone correlated negatively with mI and positively with NAA (65).

Table 2. ^{1}H-MRS studies of brain inflammatory markers in alcohol and tobacco

Authors (year) (ref.)	Study population	Substance studied	Length since last use	Brain regions	MRS marker	Group differences
Schweinsburg et al. (2000) (43)	4 recently detoxified AUD, 5 long-term abstinent AUD, 5 controls	Alcohol	Recently detoxified: 27–44 days, long-term abstinent: 5–16 years	Thalamus	NAA Cho mI	⟷ ⟷ ↑[A]
O'Neill et al. (2001) (131)	12 AUD, 13 controls	Alcohol	Mean 103 ± 72 weeks (range 3–209 weeks)	Prefrontal WM/GM, posterior parietal WM/GM	NAA Cho	↓ (All GM) ⟷
Schweinsburg et al. (2001) (132)	37 AUD, 13 controls	Alcohol	Recently detoxified, mean 27.9 ± 11.0 days	Frontal WM, parietal WM	NAA Cho mI	↓ (Frontal WM) ⟷ ↑ (Average of ROIs)
Bendszus et al. (2001) (133)	21 inpatient AUD, 12 controls	Alcohol	1–3 and 36–39 days	Frontal lobe, Cb	NAA/Cre Cho/Cre	↓[A] ↓[A] (Cb)
Parks et al. (2002) (134)	31 inpatient AUD, 12 controls	Alcohol	3–5 days, 3 weeks, and 3 months	Frontal lobe, Cb	NAA Cho mI	↓ (Cb) ↓ (Cb) ⟷
Bloomer et al. (2004) (135)	12 heavy drinkers, 10 light drinkers	Alcohol	Current drinkers	Midbrain/pons	NAA/Cre Cho/Cre	↓ ↓
Durazzo et al. (2004) (53, 136)	24 outpatient AUD, 26 controls	Alcohol	Mean 6 ± 3 and 34 ± 10 days	Frontal WM/GM, parietal WM/GM, temporal WM/GM, occipital WM, thalamus, caudate, midbrain, Cb	NAA Cho mI	↓[B] ↓[C]
Meyerhoff et al. (2004) (137)	46 heavy drinkers, 52 light drinkers	Alcohol	Current drinkers	Frontal WM/GM, parietal WM/GM, brain stem, thalamus	NAA Cho mI	↓ (Frontal WM) ↓ (Parietal GM) ⟷
Ende et al. (2005) (138)	33 inpatient AUD, 30 controls	Alcohol	4–27 days, 3 months, and 6 months	Cb, dlPFC, dentate nucleus, frontal WM, superior frontal gyrus	NAA Cho	↓[A] (Frontal WM) ↓[A] (Cb/frontal WM)
Mason et al. (2006) (139)	12 inpatient AUD, 8 controls	Alcohol	1 week and 1 month	Occipital cortex	NAA Cho	⟷ ⟷
Lee et al. (2007) (140)	13 inpatient AUD, 18 controls	Alcohol	≥2 weeks, average 15 days	ACC, insula	NAA Cho mI	⟷ ↓ (ACC) ⟷
Thoma et al. (2011) (141)	10 active AUD, 7 abstinent AUD, 23 controls	Alcohol	Active: active drinkers, abstinent: >1 year	Medial frontal/cingulate cortex	NAA Cho mI	⟷ ⟷ ⟷
Modi et al. (2011) (142)	9 AUD, 13 controls	Alcohol	1 week	Occipital lobe	NAA/Cre Cho/Cre	⟷ ↓
Mon et al. (2012) (143)	44 outpatient AUD, 16 controls	Alcohol	1 and 5 weeks	ACC, dlPFC, parieto-occipital cortex	NAA Cho mI	↓[A] (ACC) ⟷ ⟷
Hermann et al. (2012) (144)	47 inpatient AUD, 57 controls	Alcohol	1 and 14 days	ACC	NAA Cho mI	↓[A] ⟷ ⟷
Xia et al. (2012) (145)	49 AUD, 45 controls	Alcohol	Current drinkers	Prefrontal WM/GM, parietal WM/GM, Cb	NAA/Cre	↓ (Prefrontal WM/GM)
Yeo et al. (2013) (146)	213 AUD, 66 controls	Alcohol	≥24 hours	Medial frontal cortex	NAA Cho mI	⟷ ⟷ ⟷
Ende et al. (2013) (147)	23 heavy drinkers, 9 light drinkers	Alcohol	Current drinkers	Frontal WM	NAA Cho mI	⟷ ↑ ⟷
Abé et al. (2013) (148)	40 AUD, 16 controls	Alcohol	1 month	ACC, dlPFC, parieto-occipital cortex	NAA Cho mI	⟷ ⟷ ⟷
Bauer et al. (2013) (149)	29 inpatient AUD, 31 controls	Alcohol	≥24 hours of termination of medication for withdrawal symptoms but <10 days	ACC, Nac	NAA, Cho, mI Cho mI	⟷ ⟷ ⟷
Silveri et al. (2014) (150)	21 binge drinkers, 27 light drinkers	Alcohol	Active drinkers	ACC, parieto-occipital cortex	NAA	↓(ACC)
Bagga et al. (2014) (151)	35 AUD, 35 controls	Alcohol	>2 weeks, mean 17.5 days	Primary visual cortex	NAA/Cre Cho/Cre mI/Cre	↑ ↑ ↓
Zahr et al. (2016) (41)	20 AUD, 15 controls	Alcohol	Mean 20 ± 13 days	Frontal WM, Thalamus	NAA Cho	⟷ ⟷
Frischknecht et al. (2017) (42)	39 inpatient AUD, 34 controls	Alcohol	1 day and 2 weeks	Hippocampus	NAA	↓[B]
de Souza et al. (2018) (152)	22 outpatient AUD, 23 controls	Alcohol	≥15 days, mean 45 ± 37 days	Left and right PFC	Cho/Cre	↓ (LPF)
Prisciandaro et al. (2019) (153)	20 NTS AUD, 20 controls	Alcohol	1–5 days	ACC	NAA/water Cho/water mI/water	⟷ ⟷ ⟷
Grecco et al. (2021) (154)	16 AUD, 14 controls	Alcohol	>12 hours	ACC	NAA/Cre Cho/Cre mI/Cre	⟷ ⟷ ⟷
Gallinat et al. (2007) (52)	13 smokers, 13 nonsmokers	Tobacco	Current smokers	Hippocampus, ACC	NAA Cho	↓ (Hippocampus) ⟷
Mennecke et al. (2014) (50)	12 smokers, 12 nonsmokers	Tobacco	Before and day 3 of withdrawal	Hippocampus, ACC	NAA/Cre Cho/Cre mI/Cre	⟷ ↓ (Left ACC) ⟷
Durazzo et al. (2016) (47)	35 smokers, 30 nonsmokers	Tobacco	Current smokers	ACC, dlPFC	NAA Cho mI	↓ (dlPFC) ⟷ ↓ (dlPFC)
Schulte et al. (2017) (155)	30 smokers, 61 nonsmokers	Tobacco	Current smokers	ACC	NAA	⟷
Faulkner et al. (2020) (51)	44 smokers, 42 nonsmokers	Tobacco	Current smokers	Right mPFC	NAA Cho mI	↓ ⟷ ↓
Steinegger et al. (2021) (156)	29 smokers, 25 nonsmokers	Tobacco	Satiated, >30 minutes, and >24 hours	Nac	NAA Cho mI + glycine	⟷ ⟷ ↓
Bagga et al. (2021) (157)	20 smokers, 20 nonsmokers	Tobacco	Current smokers, abstain >1 hour before scan	PFC	NAA/Cre Cho/Cre mI/Cre	⟷ ↓ ⟷

Arrows in the group differences column indicate whether there was a higher level of metabolites in the SUD population than in controls (↑), a lower level of metabolites in the SUD population than in controls (↓), or no difference between groups (⟷). [A]Only during early withdrawal/abstinence. [B]Frontal white matter/gray matter during short abstinence and parietal white matter during 1-month abstinence. [C]Frontal white matter/gray matter, parietal white matter, and thalamus during short abstinence, but only parietal white matter and thalamus during 1-month abstinence. ACC, anterior cingulate cortex; AUD, alcohol use disorder; BG, basal ganglia; Cb, cerebellum; Cre, creatine; Cho, choline; dlPFC, dorsolateral prefrontal cortex; GM, gray matter; mI, myo-inositol; mPFC, medial prefrontal cortex; Nac, nucleus accumbens; NAA, N-acetyl aspartate; PFC, prefrontal cortex; WM, white matter.

Table 3. ^{1}H-MRS studies of brain inflammatory markers in other SUDs

Authors (year) (ref.)	Study population	Substance studied	Length since last use	Brain regions	MRS marker	Group differences
O'Neill et al. (2001) (131)	8 CUD, 13 controls	Cocaine	Mean 9 ± 12 weeks (range 5–34 weeks)	Prefrontal WM/GM, posterior parietal WM/GM	NAA Cho	⟷ ⟷
Ke et al. (2004) (158)	35 CUD, 20 controls	Cocaine	Not specified	Left PFC	NAA Cho	⟷ ⟷
Yang et al. (2009) (159)	14 CUD, 14 controls	Cocaine	Current users	ACC	NAA/Cre Cho/Cre mI/Cre	⟷ ⟷ ⟷
Martinez et al. (2014) (160)	15 CUD, 14 controls	Cocaine	Current users	Striatum	NAA/water Cho/water	⟷ ⟷
Hulka et al. (2014) (161)	13 CUD, 18 controls	Cocaine	>3 days, mean 8 ± 7 days	ACC, dlPFC	NAA/Cre Cho/Cre mI/Cre	⟷ ↑ ⟷
Crocker et al. (2017) (162)	21 abstinent CUD, 30 controls	Cocaine	>7 days, average 187 ± 251 days (range 15–1,432 days)	PFC	NAA Cho	↓ ⟷
Ernst et al. (2000) (163)	26 MUD, 24 controls	Methamphetamine	>2 weeks, mean 4 months (range 0.5–21 months)	Frontal GM, right frontal WM, right BG	NAA Cho mI	↓ (BG and frontal WM) ↑ (Frontal GM) ↑ (Frontal GM)
Nordahl et al. (2002) (164)	9 MUD, 9 controls	Methamphetamine	4–13 weeks	ACC, ventrolateral prefrontal WM, dorsolateral prefrontal WM, primary visual cortex	NAA/Cre Cho/Cre	↓(ACC) ⟷
Chang et al. (2005) (165)	36 MUD/HIV$^-$, 24 MUD/HIV$^+$, 44 HIV$^+$, 39 controls	Methamphetamine	>1 weeks, HIV$^-$: mean 5 ± 6 months, HIV$^+$: mean 6 ± 8 months	Frontal WM/GM, BG	NAA Cho mI	↓ (BG and frontal WM) ↑ (Frontal GW) ↑ (Frontal GW)
Sung et al. (2007) (166)	30 MUD, 20 controls	Methamphetamine	>4 weeks, mean 783 ± 1,322 days	Midfrontal GM, left frontal WM	NAA Cho mI	⟷ ⟷ ↑ (Frontal WM)
Salo et al. (2007) (56)	36 MUD, 16 controls	Methamphetamine	>3 weeks	ACC, primary visual cortex	NAA/Cre Cho/Cre	↓ (ACC) ⟷
Salo et al. (2011) (58)	30 MUD short-term abstinence, 17 MUD long-term abstinence, 24 controls	Methamphetamine	Short-term abstinence: 1–6 months, long-term abstinence: 1–5 years	ACC, primary visual cortex	NAA/Cre Cho/Cre	↓^{B} (ACC) ⟷
Salo et al. (2011) (167)	32 MUD, 13 controls	Methamphetamine	>3 weeks, mean 20 ± 5 months	ACC, primary visual cortex	NAA/Cre Cho/Cre	↓(ACC) ⟷
Sung et al. (2013) (168)	9 MUD, 10 controls	Methamphetamine	Not specified	Midfrontal lobe	NAA/Cre Cho/Cre mI/Cre	⟷ ⟷ ⟷
Howell et al. (2014) (169)	16 MUD, 10 methamphetamine-induced psychosis, 19 controls	Methamphetamine	MUD: mean 56 ± 60 days (range 1–240 days), psychosis: mean 60 ± 52 days (range 1–108 days)	ACC, frontal WM, dlPFC	NAA/Cre Cho/Cre mI/Cre	↓ (Right ACC) ⟷ ⟷
Crocker et al. (2014) (170)	29 MUD, 45 controls	Methamphetamine	>1 weeks, median 370 days	mPFC	NAA Cho	↓ ⟷
Lin et al. (2015) (171)	18 MUD, 22 controls	Methamphetamine	Current user	BG, visual cortex	NAA/Cre Cho/Cre mI/Cre	⟷ ⟷ ⟷
Burger et al. (2018) (57)	31 MUD acute abstinence, 22 MUD short-term abstinence, 22 controls	Methamphetamine	Acute: mean 1.5 ± 0.6 weeks, short-term: mean 5 ± 1 weeks	ACC, dlPFC, frontal WM	NAA/Cre Cho/Cre mI/Cre	↓ (Left DLPFC) ↓ (Left frontal WM) ↑^{A} (Right ACC)
Su et al. (2020) (172)	50 MUD, 20 controls	Methamphetamine	Not specified	dlPFC	NAA Cho mI GSH	↓ ↓ ↓ ↑
Bakhshinezhad et al. (2022) (55)	30 MUD, 20 controls	Methamphetamine	Current user	ACC, dlPFC, BG	NAA/Cre Cho/Cre	↓ ↑
Verdejo-García et al. (2013) (65)	10 OUD on methadone, 14 OUD on buprenorphine, 24 controls	Opioids	Methadone: 8–124 months, buprenorphine: 3–64 months	ACC	NAA Cho mI	↓ ⟷ ↑^{C} (Right ACC)
Liu et al. (2017) (173)	20 OUD, 20 controls	Opioids	Not specified	Nac	NAA Cho mI	⟷ ⟷ ⟷
Chang et al. (2006) (174)	21 HIV$^+$ cannabis users, 24 HIV$^-$ cannabis users, 21 HIV$^+$ individuals, 30 controls	Cannabis	HIV$^-$: mean 52 ± 17 months (range 0–240 months), HIV$^+$: mean 22 ± 9 months (range 0–132 months)	BG	mI	↓
Silveri et al. (2011) (175)	15 cannabis dependence, 11 controls	Cannabis	Current user	BG, thalamus, temporal and parietal lobes, occipital WM/GM	NAA/Cre Cho/Cre mI/Cre	⟷ ⟷ ↓
Prescot et al. (2011) (63)	17 adolescent cannabis users, 17 controls	Cannabis	Not specified	ACC	NAA/water Cho/water mI/water	↓ ⟷ ↑
Muetzel et al. (2013) (61)	27 cannabis users, 26 controls	Cannabis	Current user	BG	mI	↑ In female users only
Mashhoon et al. (2013) (64)	13 cannabis users, 10 controls	Cannabis	Current user	Thalamus	mI	↓

Arrows in the group differences column indicate whether there was a higher level of metabolites in the SUD population than in controls (↑), a lower level of metabolites in the SUD population than in controls (↓), or no difference between groups (⟷). ^{A}Only during early withdrawal/abstinence. ^{B}Frontal white matter/gray matter during short abstinence and parietal white matter during 1-month abstinence. ^{C}Only in OUD individuals maintained on buprenorphine. ACC, anterior cingulate cortex; BG, basal ganglia; Cb, cerebellum; Cre, creatine; Cho, Choline; dlPFC, dorsolateral prefrontal cortex; CUD, cocaine use disorder; GM, gray matter; GSH, glutathione; mI, myo-inositol; mPFC, medial prefrontal cortex; MUD, methamphetamine use disorder; Nac, nucleus accumbens; NAA, N-acetyl aspartate; OUD, opioid use disorder; PFC, prefrontal cortex; WM, white matter.

MRI: diffusion tensor imaging

Diffusion-tension imaging (DTI) is an MRI technique that measures the motion and diffusion of water molecules within tissues and assesses white matter microstructures. Fractional anisotropy (FA) is calculated from DTI and indexes the nonuniformity of water diffusion. High FA reflects selective diffusion along specific directions due to the presence of impermeable or semipermeable walls in the white matter (66). Although FA is not a direct marker of neuroinflammation, low FA may be indicative of demyelination, axonal loss, and blood-brain barrier permeability in neuroinflammatory conditions (66, 67).

Alcohol. An analysis of 25,378 participants from the UK Biobank reported a negative correlation between weekly alcohol intake and FA in the corpus callosum and fornix (68, 69). Furthermore, case-control studies consistently show lower FA in individuals with AUD compared with healthy controls, suggestive of aberrations in brain white matter microstructure and neuroinflammation with chronic alcohol consumption (Table 3). During early abstinence (2–3 weeks) FA was further diminished (70), but longer-term abstinence tended to increase FA, especially in the right cingulum and hippocampus (71, 72). In contrast, Fortier et al. (73) found widespread reductions in FA, including in frontal, temporal, parietal, and cerebellar white matter in individuals with AUD with an average of 25 years of misuse compared with controls following 5 years of alcohol abstinence (Table 4).

Low FA may have neuropsychological consequences that impact AUD treatment outcomes. Monnig et al. (74) associated lower FA with greater conditioned brain response to alcohol cues in the frontoparietal and corticothalamic networks, as measured by functional MRI. Lower FA in the corpus callosum and corona radiata has also been associated with greater impulsivity and poorer decision-making in individuals with AUD (75, 76). Finally, FA measurements have been shown to predict relapse in individuals with AUD: those who relapsed 1 (77) or 6 months (78) after treatment had lower baseline FA in the corpus callosum (77), frontal white matter tract (78), and stria terminalis (77) than those who successfully abstained from alcohol.

Tobacco. Studies comparing FA between smokers and nonsmokers have shown inconsistent results (Table 5). One study reported increased FA in the prefrontal white matter, cingulum, and corpus callosum (79), while another found lower FA in the cingulum of smokers compared with nonsmokers (80). Interestingly, both studies found a negative association between FA and tobacco exposure in these distinct regions (79, 80). One possible explanation that reconciles these inconsistencies is that tobacco smoking increases FA in early adulthood, which then declines with continual smoking in later life (81).

Stimulants. A meta-analysis in individuals with stimulant use disorder (i.e., CUD and MUD) showed lower FA compared with controls in the corpus callosum, particularly the genu, and the frontal white matter, all with small-to-moderate effects (82). Studies examining FA in individuals with MUD are listed in Table 5 and generally reported either lower FA compared with controls or no group differences. Low FA was found to contribute to impaired performance on neurocognitive tasks (e.g., performance on the Stroop Attention Test or Wisconsin Card Sorting Test) in individuals with MUD (83, 84).

A meta-analysis showed lower FA in CUD than control individuals in the corpus callosum with small-to-moderate effect size, and in the anterior thalamic projections and striatum at the level of a trend (85). Several studies associated lower FA with higher impulsivity (86, 87) and altered reward signaling (88), which have been thought to contribute to poorer CUD treatment outcomes. In treatment-seeking individuals with CUD, higher baseline FA prior to treatment initiation was positively associated with a longer duration of abstinence (89). He et al. (90) found low FA in the frontal cortical tracts (e.g., corpus callosum, superior longitudinal fasciculus, and inferior frontal-occipital fasciculus) and the frontal white matter in individuals with current but not past CUD, suggesting that abstinence may restore FA levels.

Opioids. Multiple studies found lower FA in individuals with OUD compared with healthy controls (Table 5), except for Sun et al. (91) who reported higher FA. Specifically, a meta-analysis of extant literature reported low FA in the frontal subgyral area, including the cingulum and superior longitudinal fasciculus in individuals with OUD compared with controls (92). Exposure to methadone contributed to, but did not fully account for low FA (93), as individuals with OUD who were not maintained on medications for treating OUD (methadone and buprenorphine) also showed low FA (94). In a comparison of individuals with fewer than 10 years or 10–20 years of heroin use, a longer duration of opioid exposure was associated with more widespread reductions in FA, particularly in the corpus callosum, thalamic radiation, and parietal, frontal, and temporal tracts (95). Cessation of opioid use partially restored FA measures (96, 97).

Several studies associated lower FA with impaired decision-making and impulsivity on the Iowa Gambling Task (95, 98). Furthermore, another study reported a negative relationship between FA in the frontostriatal tract and opioid craving in individuals with OUD (96). The role of FA in these neuropsychological domains could have implications for treatment outcomes. In individuals undergoing methadone treatment, those who relapsed after 6 months demonstrated lower FA in the internal and external capsules and the corona radiata than those who were abstinent (99).

MRI: linking peripheral inflammatory markers and brain function

Chronic inflammation contributes to neurodegeneration in normal aging and neurodegenerative diseases, including Alzheimer's and Parkinson's disease (100–102). Peripheral inflammatory markers (i.e., white blood cells, high-sensitivity C-reactive protein, and fibrinogen) were found to associate with brain signatures of aging, including reduced total brain and gray matter volume (103). Similarly, several studies, as summarized below, have shown that inflammatory markers mediate the neurobiological consequences of substance misuse.

Alcohol. Increased intestinal permeability due to alcohol consumption may lead to the leakage of proinflammatory LPS into the systemic circulation, triggering an inflammatory cascade. In comparison with healthy controls, individuals with AUD showed intestinal hyperpermeability, higher plasma LPS concentrations, and higher levels of the proinflammatory cytokines TNF-α and IL-8 (104), which correlated positively with alcohol craving, suggesting a gut-brain interaction in individuals with AUD (104). TLR4 is a

Table 4. MRI studies of fractional anisotropy in alcohol and tobacco

Authors (year) (ref.)	Study population	Substance studied	Length since last use	Change in FA
Pfefferbaum & Sullivan (2002) (176)	27 AUD, 41 controls	Alcohol	Female: median 677 days (range 49–2,384 days), male: median 332 days (range 25–5,110 days)	↓
Pfefferbaum et al. (2006) (177, 178)	57 AUD, 74 controls	Alcohol	Male: mean 98 ± 118 days, female: mean 76 ± 93 days	↓
De Bellis et al. (2008) (179)	32 AUD, 28 controls	Alcohol	Mean 63.7 ± 88.2 days	↑
Chanraud et al. (2008) (180)	20 outpatient AUD, 24 controls	Alcohol	>3 weeks, mean 29 ± 34 weeks	⟷
Yeh et al. (2009) (181)	11 outpatient AUD, 10 controls	Alcohol	Mean 6 ± 3 days	↓
Gazdzinski et al. (2010) (54)	36 outpatient AUD, 22 controls	Alcohol	Mean 6 ± 3 and 32 ± 9 days	⟷
Konrad et al. (2012) (182)	24 inpatient AUD, 23 controls	Alcohol	6–20 days after withdrawal pharmacotherapy	↓
Alhassoon et al. (2012) (71)	15 AUD, 15 controls	Alcohol	2 weeks and 1 year	↓
Zorlu et al. (2013) (183)	17 inpatient AUD, 16 controls	Alcohol	> 2 weeks	↓
Bagga et al. (2014) (184)	35 AUD, 30 controls	Alcohol	Mean 17 ± 4 days	↓
Zorlu et al. (2014) (185)	12 AUD, 13 controls	Alcohol	>6 months, mean 28 months	⟷
Fortier et al. (2014) (73)	31 AUD, 20 controls	Alcohol	>1 month, mean 5 ± 8 years	↓
Wang et al. (2016) (75)	20 AUD, 20 controls	Alcohol	Mean 42 ± 11 days	↓
Zou et al. (2017) (72)	20 short abstinent AUD, 52 long abstinent AUD, 20 controls	Alcohol	Short abstinent: 1 week, long abstinent: 1 month	↓
Chumin et al. (2018) (186)	38 NTS AUD, 19 controls	Alcohol	Current use	↓
Sawyer et al. (2018) (187)	49 AUD, 41 controls	Alcohol	Women: mean 9 ± 10 years, men: mean 5 ± 8 years	↓(males) ↑(females)
Pandey et al. (2018) (188)	30 AUD, 30 controls	Alcohol	>5 days, mean 673 ± 845 days	↓[A]WM regions ↑ Thalamus
De Santis et al. (2019) (70)	91 inpatient AUD, 36 controls	Alcohol	1 week	↓
Crespi et al. (2020) (76)	22 inpatient AUD, 18 controls	Alcohol	>10 days of detoxification, ceasing benzodiazepine for at least 8 days	↓
Wiers et al. (2020) (189)	15 AUD, 14 controls	Alcohol	Mean 3.5 days (range 1–7 days)	↓ Thalamus ⟷ ACC
Bracht et al. (2021) (190)	39 inpatient AUD, 18 controls	Alcohol	>4 weeks, mean 30 ± 15 days	↓
Lee et al. (2021) (191)	23 inpatient AUD, 22 controls	Alcohol	13 ± 17 months	↓
Kisner et al. (2021) (192)	100 inpatient AUD, 98 controls	Alcohol	6–44 days	↓
Yoder et al. (2023) (193)	13 NTS AUD, 30 controls	Alcohol	Not specified	↓
Wu et al. (2023) (194)	51 AUD, 27 controls	Alcohol	2–4 weeks	↓
Paul et al. (2008) (195)	10 smokers, 10 nonsmokers	Tobacco	Current smoker	↑
Zhang et al. (2011) (196)	48 smokers, 48 nonsmokers	Tobacco	Current smoker, abstain for >2 hours before the scan	⟷ (Whole brain) ↓ (PFC)
Liao et al. (2011) (197)	44 smokers, 44 nonsmokers	Tobacco	Current smoker, abstain for >12 hours before the scan	↑
Hudkins et al. (2012) (79)	18 smokers, 18 nonsmokers	Tobacco	Current smoker	↑
Lin et al. (2013) (198)	34 smokers, 34 nonsmokers	Tobacco	Current smoker	↓
Umene-Nakano et al. (2014) (199)	19 smokers, 18 nonsmokers	Tobacco	Current smoker	↓
Savjani et al. (2014) (200)	30 smokers, 32 nonsmokers	Tobacco	Current smoker, abstain for > 24 hours before the scan	↓
Yu et al. (2016) (201)	23 smokers, 22 nonsmokers	Tobacco	Current smoker	↑
Baeza-Loya et al. (2016) (80)	31 smokers, 39 nonsmokers	Tobacco	Current smoker, abstain for >12 hours before the scan	↓
Li et al. (2017) (202)	31 smokers, 30 nonsmokers	Tobacco	Current smoker, smoked <1 hours before the scan	↑
Wang et al. (2017) (203)	19 smokers, 23 nonsmokers	Tobacco	Current smoker, abstain for >2 hours before the scan	↑
Bi et al. (2017) (204)	35 smokers, 26 nonsmokers	Tobacco	Current smoker, smoked ~1 hours before the scan	↑
Yuan et al. (2018) (205)	36 smokers, 35 nonsmokers	Tobacco	Current smoker, smoked ~1 hours before the scan	↓
Bagga et al. (2018) (206)	28 smokers, 28 nonsmokers	Tobacco	Current smoker, smoked >0.5 hours before the scan	↑
Kangiser et al. (2020) (207)	18 smokers, 35 nonsmokers	Tobacco	Current smoker	↓
Hunag et al. (2020) (208)	156 smokers, 81 nonsmokers	Tobacco	Current smoker	↓
Wang et al. (2020) (209)	58 smokers, 34 controls	Tobacco	Current smoker	↓↑[A]
Zhou et al. (2022) (210)	37 smokers, 29 controls	Tobacco	Current smoker	↓↑[A]

Arrows in the group differences column indicate whether there was higher FA in the SUD population than in controls (↑), lower FA in the SUD population than in controls (↓), or no difference between groups (⟷). [A]Voxel-wise analyses showed ↓↑ in different brain regions. AUD, alcohol use disorder; NTS, nontreatment seeking.

pattern recognition receptor that identifies pathogens and triggers inflammatory responses. Methylation of the *TLR4* gene moderated the relationship between alcohol use severity and brain gray matter volume, such that greater alcohol severity was associated with lower precuneus and inferior parietal gray volumes in individuals with low (but not high) methylation (105).

Table 5. MRI studies of fractional anisotropy in other SUDs

Authors (year) (ref.)	Study population	Substance studied	Length since last use	Change in FA
Lim et al. (2002) (211)	12 CUD, 13 controls	Cocaine	Current user	↓
Moeller et al. (2004) (87)	18 CUD, 18 controls	Cocaine	Current user	↓
Lim et al. (2008) (212)	18 CUD, 18 controls	Cocaine	> 4 days	↓
Ma et al. (2010) (213)	19 CUD, 18 controls	Cocaine	Current user	↓↑[A]
Romero et al. (2010) (86)	32 outpatient CUD, 33 controls	Cocaine	>72 hours	↓↑[A]
Lane et al. (2010) (214)	15 CUD, 18 controls	Cocaine	Not specified	↓
Bell et al. (2011) (215)	43 abstinent inpatient or outpatient CUD, 43 controls	Cocaine	Short-term abstinent: 0.7–5.1 weeks, midterm abstinent: 10–40.3 weeks, long-term abstinent: 44–102 weeks	↓↑[A]
Ma et al. (2015) (98)	12 CUD, 12 controls	Cocaine	Not specified	↓
Vaquero et al. (2017) (88)	30 detoxified inpatient CUD, 30 controls	Cocaine	Not specified	↓↑[A]
Ma et al. (2017) (216)	11 treatment seeking CUD, 11 control	Cocaine	Baseline and 10 weeks of a treatment study	⟷
He et al. (2020) (90)	12 current CUD, 20 abstinent CUD, 7 controls	Cocaine	Abstinent: 1–5 years, 6–10 years, or 11+ years	↓ (Current CUD only)
Tondo et al. (2021) (217)	75 inpatient CUD, 58 controls	Cocaine	Not specified	↓
Meade et al. (2021) (218)	35 CUD, 37 controls	Cocaine	Current user	↓
Ottino-González et al. (2022) (219)	154 CUD, 333 controls	Cocaine	<1 year	↓
Gaudreault et al. (2023) (220)	28 current CUD, 32 abstinent CUD, 58 controls	Cocaine	Abstinent: mean 18 months	↓
Hodges et al. (2023) (221)	25 CUD, 21 controls	Cocaine	Current user	↓
Chung et al. (2007) (222)	32 MUD, 30 controls	Methamphetamine	> 4 weeks, mean 24 ± 38 months	↓
Salo et al. (2009) (84)	37 MUD, 17 controls	Methamphetamine	>3 weeks, mean 21 ± 32 months (range 3 weeks to 10 years)	⟷
Kim et al. (2009) (83)	11 MUD, 13 controls	Methamphetamine	Mean 18 ± 7	↓
Alicata et al. (2009) (223)	30 MUD, 30 controls	Methamphetamine	Mean 140 ± 400 days (range 0–1,798 days)	↓
Tobias et al. (2010) (224)	23 MUD, 18 controls	Methamphetamine	7–13 days	↓
Daumann et al. (2011) (225)	20 experienced users, 42 low-exposure users, 16 controls	Methamphetamine	Experienced: mean 142 ± 484 days, low-exposure: mean 393 ± 808 days	⟷
Lederer et al. (2015) (226) and Uhlmann et al. (2016) (227)	40 MUD, 40 controls	Methamphetamine	Median 21 (range 1–240 days)	⟷
Andres et al. (2016) (228)	32 past users, 27 current users, 35 controls	Methamphetamine	Past: >30 days, current: <30 days	↑ (Past users)
Li et al. (2017) (229, 230)	28 MUD, 28 controls	Methamphetamine	Not specified	↓
Ottino-González et al. (2022) (219)	132 MUD, 333 controls	Methamphetamine	Not specified	↓
Zhou et al. (2023) (231)	69 MUD, 47 controls	Methamphetamine	Mean 62 ± 40 days	⟷
Liu et al. (2009) (232)	16 OUD, 16 controls	Opioids	Received methadone maintenance treatment for mean 4 ± 1 day	↓
Bora et al. (2010) (233)	24 OUD, 29 controls	Opioids	Weekly opioid use in the previous 3 months	↓
Wang et al. (2011) (93)	13 methadone-treated OUD, 11 abstinent OUD, 15 controls	Opioids	Methadone: received treatment for at least 3–9 months, mean 5 ± 1 month; abstinent: 5–8 months, mean 7 ± 1 month	↓ (Methadone-treated only)
Wang et al. (2011) (234)	20 OUD, 20 controls	Opioids	3 days and 1 month	↓[B]
Shen et al. (2012) (97)	18 short-term abstinent OUD, 17 long-term abstinent OUD, 17 controls	Opioids	Short-term: mean 1 ± 0.3 months; long-term: mean: 14 ± 2 months	↓
Qiu et al. (2013) (95)	18 short-term OUD, 18 long-term OUD, 16 controls	Opioids	Not specified	↓
Li et al. (2013) (94)	17 OUD, 15 controls	Opioids	Mean 8 ± 2 days	↓
Ma et al. (2015) (235)	14 OUD, 14 controls	Opioids	Not specified	↓
Sun et al. (2015) (91)	76 OUD, 78 controls	Opioids	1 month to 1 year	↑
Lu et al. (2022) (96)	53 OUD, 39 controls	Opioids	Mean 60 ± 69 and 306 ± 99 days	↓
Gaudreault et al. (2023) (220)	30 OUD, 58 controls	Opioids	Mean 199 ± 265 days	↓
Lu et al. (2023) (236)	42 OUD, 39 controls	Opioids	Mean 53 ± 67 and 308 ± 119 days	↓[B]

Arrows in the group differences column indicate whether there was higher FA in the SUD population than in controls (↑), lower FA in the SUD population than in controls (↓), or no difference between groups (⟷). [A]Voxel-wise analyses showed ↓↑ in different brain regions. [B]Only in early withdrawal/abstinence. CUD, cocaine use disorder; MUD, methamphetamine use disorder; OUD, opioid use disorder.

Stimulants. Higher levels of IL-6 but not IL-1β or IL-10 were found in individuals with MUD compared with healthy controls (106), which, in individuals with MUD, was associated with disruptions in striatal-limbic and cortico-striatal resting-state functional connectivity (106).

Opioids. In individuals with OUD, 12 weeks of methadone treatment significantly decreased plasma cytokine levels and improved behavioral performance on a memory task (107). These changes in inflammatory markers and memory capacity were strongly correlated: the concentration of TNF-α correlat-

ed negatively with visual memory capacity, and concentration of IL-6 correlated negatively with verbal memory and decayed recall indices (107). A follow-up study also associated higher IL-6 levels during methadone treatment with poorer medication compliance and drop-out (108), reflecting adverse effects of neuroinflammation on real-life behaviors. In concert, findings from these studies highlight the role of inflammation in neural functioning and its potential implications for OUD treatment outcomes.

Discussion and future directions

Here, we reviewed the human literature on PET and MRI markers of neuroinflammation in SUDs. PET studies with tracers that bind to TSPO, a marker of microglial activation, demonstrated consistent upregulation in response to neuroimmune challenges (109) and to acute alcohol administration (26). However, differential effects have been reported in SUDs. Chronic alcohol exposure in individuals with AUD is consistently associated with lower TSPO than in nondependent controls (meta-analyzed in ref. 18), suggesting temporal dynamics of acute inflammatory insults versus downregulation of TSPO in response to chronic alcohol exposure. Tobacco smoking was also associated with low brain TSPO levels in two of three studies, whereas cocaine, methamphetamine, and cannabis users were found either to have higher brain TSPO levels than controls or to show no significant differences. Current PET studies in SUD are limited by TSPO nondisplaceable binding and competition from metabolites involved in essential mitochondrial functions (e.g., cholesterol transport). Future research with longitudinal designs or new promising PET radiotracers could elucidate the effects of SUD on neuroimmune signaling. For example, newer PET tracers that target COX-1 and COX-2 or inducible nitric oxide synthase (iNOS) were found to be sensitive to neuroinflammation in individuals with Alzheimer's disease (110), Parkinson's disease (111), and lung inflammation in electronic cigarette users (112). These tracers may be promising for detecting neuroinflammation in SUDs. Furthermore, MRI research on inflammation consistently showed increased levels of mI in brain, measured using ^{1}H-MRS (e.g., meta-analyzed in 39), and lower FA in drug users compared with controls. However, these MRI measures do not directly assess neuroinflammation markers but rather downstream consequences (e.g., neuronal dysfunction, membrane turnover, and white matter microstructure). Future studies that combine PET and MRI modalities and associate them with peripheral markers of inflammation will help to clarify the role of neuroinflammation in modulating drug reward and the neuroadaptations resulting from acute drug administration, chronic drug exposure, and treatment for SUDs.

Several antiinflammatory medications have shown promise as treatment options for SUD. These include medications that target phosphodiesterases (PDEs), which comprise a large family of enzymes that regulate intracellular levels of secondary messengers, cAMPs, which are subsequently involved in the initiation and progression of inflammatory pathways. Inhibition of PDEs with the medications apremilast and ibudilast decreased markers of inflammation (113–115) as well as alcohol craving and consumption in preclinical and clinical studies (116–118). Preclinical studies also found that ibudilast treatment attenuated cocaine and methamphetamine self-administration in rodents (119, 120). Among non-treatment-seeking individuals with OUD, ibudilast attenuated subjective liking for oxycodone and reduced oxycodone self-administration (121). However, in treatment-seeking individuals with MUD, the effects on methamphetamine abstinence did not differ between those of ibudilast and placebo (122). Further elucidation of the clinical and neurobiological implications of treating SUD with ibudilast is warranted. Findings that apremilast decreases excessive drinking in individuals with AUD require replication (117). It should be noted that, in addition to modulating inflammatory pathways, PDE/cAMP signaling also regulates dopamine transmission (123), which may have contributed to ibudilast or apremilast's effects on SUD. In a preclinical study, administration of PDE4 inhibitor rolipram mitigated cocaine-induced disruption in the balance between dopaminergic excitation/inhibition in the VTA and attenuated behavioral responses to cocaine (124). Therefore, future studies are warranted to better delineate the mechanisms underlying the actions of PDE inhibitors in SUD. The radioligand ^{18}F-PF-06445974 was recently developed to quantify PDE isozyme 4B (PDE4B) (125), and it may be ideal for evaluating the effects of apremilast and ibudilast in individuals with SUD. Furthermore, N-acetyl cysteine (NAC), an antioxidant that has antiinflammatory properties and modulates glutaminergic signaling, is also being studied for the treatment of SUD (126). Preclinical studies have shown NAC to be effective in reducing drug-seeking behaviors (127), but clinical findings have been inconclusive. In a clinical trial conducted in individuals with AUD, NAC did not significantly differ from placebo in reducing alcohol consumption (128), whereas in a larger sample of individuals with cannabis use disorder, NAC administration was associated with increased odds of weekly alcohol abstinence and fewer drinking days in comparison to placebo (129). Future PET and MRI clinical treatment trials in individuals with SUDs that capture both the clinical and neuroimaging effects of antiinflammatory drug treatments are warranted.

Acknowledgments

Authors were supported by the following US NIH grants: T32DA028874 (to XL), AA026892 (to CEW), DA051709 (to ZS), and DA046345 (to CEW). Support was also provided by the following Brazilian grants: CAPES PrInt UNIFESP process: 88887.695808/2022-00 (to LSPR) and Fundação de Amparo à Pesquisa do Estado de São Paulo (FAPESP) processes: 2021/13092-7 (to LSPR).

We thank Victoria Brown for the helpful discussions and Sandhitsu Das and Christopher Brown for providing the DTI FA image.

Address correspondence to: Corinde E. Wiers, 3535 Market Street, Philadelphia, Pennsylvania, USA. Phone: 1.215.746.1898; Email: corinde.wiers@pennmedicine.upenn.edu. Or to: Nora D. Volkow, 10 Center Drive, Bethesda, Maryland 20892, USA. Phone: 1.301.402.0868; Email: nvolkow@nida.nih.gov.

1. Substance Abuse and Mental Health Services Administration. Key substance use and mental health indicators in the United States: Results from the 2021 National Survey on Drug Use and Health (HHS Publication No. PEP22-07-01-005, NSDUH Series H-57). Center for Behavioral Health Statistics and Quality, Substance Abuse and Mental Health Services Administration. 2022. https://www.samhsa.gov/data/report/2021-nsduh-annual-national-report. Updated January 4, 2023. Accessed May 21, 2020.
2. Koob GF, Volkow ND. Neurobiology of addiction: a neurocircuitry analysis. *Lancet Psychiatry*. 2016;3(8):760–773.
3. Volkow ND, Morales M. The brain on drugs: from reward to addiction. *Cell*. 2015;162(4):712–725.
4. Agarwal K, et al. Inflammatory markers in substance use and mood disorders: a neuroimaging perspective. *Front Psychiatry*. 2022;13:863734.
5. Bersano A, et al. Neuroinflammation and brain disease. *BMC Neurol*. 2023;23(1):227.
6. Gorji A. Neuroinflammation: the pathogenic mechanism of neurological disorders. *Int J Mol Sci*. 2022;23(10):5744.
7. Holloway KN, et al. Ethanol induces neuroinflammation in a chronic plus binge mouse model of alcohol use disorder via TLR4 and MyD88-dependent signaling. *Cells*. 2023;12(16):2109.
8. Pascual M, et al. Toll-like receptors in neuroinflammation, neurodegeneration, and alcohol-induced brain damage. *IUBMB Life*. 2021;73(7):900–915.
9. De Carvalho LM, et al. Increased transcription of TSPO, HDAC2, and HDAC6 in the amygdala of males with alcohol use disorder. *Brain Behav*. 2021;11(2):e01961.
10. He J, Crews FT. Increased MCP-1 and microglia in various regions of the human alcoholic brain. *Exp Neurol*. 2008;210(2):349–358.
11. Vetreno RP, et al. Increased Toll-like Receptor-MyD88-NFκB-Proinflammatory neuroimmune signaling in the orbitofrontal cortex of humans with alcohol use disorder. *Alcohol Clin Exp Res*. 2021;45(9):1747–1761.
12. Crews FT, et al. High mobility group box 1/Toll-like receptor danger signaling increases brain neuroimmune activation in alcohol dependence. *Biol Psychiatry*. 2013;73(7):602–612.
13. Wei J, et al. Single nucleus transcriptomics of ventral midbrain identifies glial activation associated with chronic opioid use disorder. *Nat Commun*. 2023;14(1):5610.
14. Zakharov S, et al. Neuroinflammation markers and methyl alcohol induced toxic brain damage. *Toxicol Lett*. 2018;298:60–69.
15. Kölliker-Frers R, et al. Neuroinflammation: an integrating overview of reactive-neuroimmune cell interactions in health and disease. *Mediators Inflamm*. 2021;2021:9999146.
16. Rupprecht R, et al. Translocator protein (18 kDa) (TSPO) as a therapeutic target for neurological and psychiatric disorders. *Nat Rev Drug Discov*. 2010;9(12):971–988.
17. Woodcock EA, et al. Imaging biomarkers of the neuroimmune system among substance use disorders: a systematic review. *Mol Neuropsychiatry*. 2019;5(3):125–146.
18. Adams C, et al. Central markers of neuroinflammation in alcohol use disorder: A meta-analysis of neuroimaging, cerebral spinal fluid, and post-mortem studies. *Alcohol Clin Exp Res (Hoboken)*. 2023;47(2):197–208.
19. Kalk NJ, et al. Decreased hippocampal translocator protein (18 kDa) expression in alcohol dependence: a [^{11}C]PBR28 PET study. *Transl Psychiatry*. 2017;7(1):e996.
20. Hillmer AT, et al. In vivo imaging of translocator protein, a marker of activated microglia, in alcohol dependence. *Mol Psychiatry*. 2017;22(12):1759–1766.
21. Kim SW, et al. Influence of alcoholism and cholesterol on TSPO binding in brain: PET [^{11}C] PBR28 studies in humans and rodents. *Neuropsychopharmacology*. 2018;43(9):1832–1839.
22. Laurell GL, et al. Nondisplaceable binding is a potential confounding factor in ^{11}C-PBR28 translocator protein PET Studies. *J Nucl Med*. 2021;62(3):412–417.
23. Tollefson S, et al. Imaging the influence of red blood cell docosahexaenoic acid status on the expression of the 18 kDa translocator protein in the brain: A [^{11}C]PBR28 positron emission tomography study in young healthy men. *Biol Psychiatry Cogn Neurosci Neuroimaging*. 2022;7(10):998–1006.
24. Jaipuria G, et al. Cholesterol-mediated allosteric regulation of the mitochondrial translocator protein structure. *Nat Commun*. 2017;8:14893.
25. Wiers CE, et al. TSPO polymorphism in individuals with alcohol use disorder: Association with cholesterol levels and withdrawal severity. *Addict Biol*. 2021;26(1):e12838.
26. Raval NR, et al. Imaging the brain's immune response to alcohol with [11C]PBR28 TSPO Positron Emission Tomography. *Molecular Psychiatry*. 2023;28:3384–3390.
27. Saba W, et al. Imaging the neuroimmune response to alcohol exposure in adolescent baboons: a TSPO PET study using ^{18} F-DPA-714. *Addict Biol*. 2018;23(5):1000–1009.
28. Brody AL, et al. Effect of cigarette smoking on a marker for neuroinflammation: A [^{11}C]DAA1106 positron emission tomography study. *Neuropsychopharmacology*. 2017;42(8):1630–1639.
29. Brody AL, et al. Effect of overnight smoking abstinence on a marker for microglial activation: a [^{11}C]DAA1106 positron emission tomography study. *Psychopharmacology (Berl)*. 2018;235(12):3525–3534.
30. Hillmer AT, et al. Tobacco smoking in people is not associated with altered 18-kDa translocator protein levels: A PET study. *J Nucl Med*. 2020;61(8):1200–1204.
31. Yoder KK, et al. Comparison of standardized uptake values with volume of distribution for quantitation of [(11)C]PBR28 brain uptake. *Nucl Med Biol*. 2015;42(3):305–308.
32. Sekine Y, et al. Methamphetamine causes microglial activation in the brains of human abusers. *J Neurosci*. 2008;28(22):5756–5761.
33. London ED, et al. No significant elevation of translocator protein binding in the brains of recently abstinent methamphetamine users. *Drug Alcohol Depend*. 2020;213:108104.
34. Rathitharan G, et al. Microglia imaging in methamphetamine use disorder: a positron emission tomography study with the 18 kDa translocator protein radioligand [F-18]FEPPA. *Addict Biol*. 2021;26(1):e12876.
35. Narendran R, et al. Cocaine abuse in humans is not associated with increased microglial activation: an 18-kDa translocator protein positron emission tomography imaging study with [11C] PBR28. *J Neurosci*. 2014;34(30):9945–9950.
36. Da Silva T, et al. In vivo imaging of translocator protein in long-term cannabis users. *JAMA Psychiatry*. 2019;76(12):1305–1313.
37. Chaney A, et al. In vivo molecular imaging of neuroinflammation in Alzheimer's disease. *J Neurochem*. 2019;149(4):438–451.
38. Rae CD. A guide to the metabolic pathways and function of metabolites observed in human brain 1H magnetic resonance spectra. *Neurochem Res*. 2014;39(1):1–36.
39. Kirkland AE, et al. Brain metabolite alterations related to alcohol use: a meta-analysis of proton magnetic resonance spectroscopy studies. *Mol Psychiatry*. 2022;27(8):3223–3236.
40. Prisciandaro JJ, et al. Associations between recent heavy drinking and dorsal anterior cingulate N-acetylaspartate and glutamate concentrations in non-treatment-seeking individuals with alcohol dependence. *Alcohol Clin Exp Res*. 2016;40(3):491–496.
41. Zahr NM, et al. Brain metabolite levels in recently sober individuals with alcohol use disorder: Relation to drinking variables and relapse. *Psychiatry Res Neuroimaging*. 2016;250:42–49.
42. Frischknecht U, et al. Negative association between MR-spectroscopic glutamate markers and gray matter volume after alcohol withdrawal in the hippocampus: a translational study in humans and rats. *Alcohol Clin Exp Res*. 2017;41(2):323–333.
43. Schweinsburg BC, et al. Elevated myo-inositol in gray matter of recently detoxified but not long-term abstinent alcoholics: a preliminary MR spectroscopy study. *Alcohol Clin Exp Res*. 2000;24(5):699–705.
44. Biller A, et al. The effect of ethanol on human brain metabolites longitudinally characterized by proton MR spectroscopy. *J Cereb Blood Flow Metab*. 2009;29(5):891–902.
45. Gomez R, et al. Intravenous ethanol infusion decreases human cortical γ-aminobutyric acid and N-acetylaspartate as measured with proton magnetic resonance spectroscopy at 4 tesla. *Biol Psychiatry*. 2012;71(3):239–246.
46. Monnig MA, et al. Cerebral metabolites on the descending limb of acute alcohol: a preliminary 1H MRS Study. *Alcohol Alcohol*. 2019;54(5):487–496.
47. Durazzo TC, et al. Chronic cigarette smoking in healthy middle-aged individuals is associated with decreased regional brain N-acetylaspartate and glutamate levels. *Biol Psychiatry*. 2016;79(6):481–488.
48. Abulseoud OA, et al. Short-term nicotine deprivation alters dorsal anterior cingulate glutamate concentration and concomitant cingulate-cortical functional connectivity. *Neuropsychopharmacology*. 2020;45(11):1920–1930.
49. Gutzeit A, et al. Insula-specific H magnetic resonance spectroscopy reactions in heavy

smokers under acute nicotine withdrawal and after oral nicotine substitution. *Eur Addict Res*. 2013;19(4):184–193.
50. Mennecke A, et al. Physiological effects of cigarette smoking in the limbic system revealed by 3 tesla magnetic resonance spectroscopy. *J Neural Transm (Vienna)*. 2014;121(10):1211–1219.
51. Faulkner P, et al. Daily and intermittent smoking are associated with low prefrontal volume and low concentrations of prefrontal glutamate, creatine, myo-inositol, and N-acetylaspartate. *Addict Biol*. 2021;26(4):e12986.
52. Gallinat J, et al. Abnormal hippocampal neurochemistry in smokers: evidence from proton magnetic resonance spectroscopy at 3 T. *J Clin Psychopharmacol*. 2007;27(1):80–84.
53. Durazzo TC, et al. Cigarette smoking exacerbates chronic alcohol-induced brain damage: a preliminary metabolite imaging study. *Alcohol Clin Exp Res*. 2004;28(12):1849–1860.
54. Gazdzinski S, et al. Chronic cigarette smoking modulates injury and short-term recovery of the medial temporal lobe in alcoholics. *Psychiatry Res*. 2008;162(2):133–145.
55. Bakhshinezhad H, et al. The relationship between brain metabolites alterations and neuropsychological deficits in patients with methamphetamine use disorder: a proton magnetic resonance spectroscopy study. *Arch Clin Neuropsychol*. 2022;37(1):160–172.
56. Salo R, et al. Attentional control and brain metabolite levels in methamphetamine abusers. *Biol Psychiatry*. 2007;61(11):1272–1280.
57. Burger A, et al. The impact of acute and short-term methamphetamine abstinence on brain metabolites: A proton magnetic resonance spectroscopy chemical shift imaging study. *Drug Alcohol Depend*. 2018;185:226–237.
58. Salo R, et al. Extended findings of brain metabolite normalization in MA-dependent subjects across sustained abstinence: a proton MRS study. *Drug Alcohol Depend*. 2011;113(2-3):133–138.
59. Christensen JD, et al. Proton magnetic resonance spectroscopy of human basal ganglia: response to cocaine administration. *Biol Psychiatry*. 2000;48(7):685–692.
60. Mason NL, et al. Reduced responsiveness of the reward system is associated with tolerance to cannabis impairment in chronic users. *Addict Biol*. 2021;26(1):e12870.
61. Muetzel RL, et al. In vivo ^{1}H magnetic resonance spectroscopy in young-adult daily marijuana users. *Neuroimage Clin*. 2013;2(1):581–589.
62. Watts JJ, et al. Evidence that cannabis exposure, abuse, and dependence are related to glutamate metabolism and glial function in the anterior cingulate cortex: A ^{1}H-magnetic resonance spectroscopy study. *Front Psychiatry*. 2020;11(1):764.
63. Prescot AP, et al. Neurochemical alterations in adolescent chronic marijuana smokers: a proton MRS study. *Neuroimage*. 2011;57(1):69–75.
64. Mashhoon Y, et al. Lower left thalamic myo-inositol levels associated with greater cognitive impulsivity in marijuana-dependent young men: preliminary spectroscopic evidence at 4T. *J Addict Res Ther*. 2013;Suppl 4:009.
65. Verdejo-García A, et al. Cingulate biochemistry in heroin users on substitution pharmacotherapy. *Aust N Z J Psychiatry*. 2013;47(3):244–249.
66. Quarantelli M. MRI/MRS in neuroinflammation: methodology and applications. *Clin Transl Imaging*. 2015;3(6):475–489.
67. Feldman DE, et al. Neuroimaging of inflammation in alcohol use disorder: a review. *Science China Information Sciences*. 2020;63(7):170102.
68. Topiwala A, et al. Alcohol consumption and MRI markers of brain structure and function: Cohort study of 25,378 UK Biobank participants. *Neuroimage Clin*. 2022;35:103066.
69. Daviet R, et al. Associations between alcohol consumption and gray and white matter volumes in the UK Biobank. *Nat Commun*. 2022;13(1):1175.
70. De Santis S, et al. Microstructural white matter alterations in men with alcohol use disorder and rats with excessive alcohol consumption during early abstinence. *JAMA Psychiatry*. 2019;76(7):749–758.
71. Alhassoon OM, et al. Callosal white matter microstructural recovery in abstinent alcoholics: a longitudinal diffusion tensor imaging study. *Alcohol Clin Exp Res*. 2012;36(11):1922–1931.
72. Zou Y, et al. Effects of abstinence and chronic cigarette smoking on white matter microstructure in alcohol dependence: Diffusion tensor imaging at 4T. *Drug Alcohol Depend*. 2017;175:42–50.
73. Fortier CB, et al. Widespread effects of alcohol on white matter microstructure. *Alcohol Clin Exp Res*. 2014;38(12):2925–2933.
74. Monnig MA, et al. White matter integrity is associated with alcohol cue reactivity in heavy drinkers. *Brain Behav*. 2014;4(2):158–170.
75. Wang J, et al. Alterations in brain structure and functional connectivity in alcohol dependent patients and possible association with impulsivity. *PLoS One*. 2016;11(8):e0161956.
76. Crespi C, et al. Microstructural damage of white-matter tracts connecting large-scale networks is related to impaired executive profile in alcohol use disorder. *Neuroimage Clin*. 2020;25:102141.
77. Zou Y, et al. White matter microstructural correlates of relapse in alcohol dependence. *Psychiatry Res Neuroimaging*. 2018;281:92–100.
78. Sorg SF, et al. Frontal white matter integrity predictors of adult alcohol treatment outcome. *Biol Psychiatry*. 2012;71(3):262–268.
79. Hudkins M, et al. Cigarette smoking and white matter microstructure. *Psychopharmacology (Berl)*. 2012;221(2):285–295.
80. Baeza-Loya S, et al. Anterior cingulum white matter is altered in tobacco smokers. *Am J Addict*. 2016;25(3):210–214.
81. Gogliettino AR, et al. White matter development and tobacco smoking in young adults: A systematic review with recommendations for future research. *Drug Alcohol Depend*. 2016;162:26–33.
82. Beard CL, et al. Regional differences in white matter integrity in stimulant use disorders: A meta-analysis of diffusion tensor imaging studies. *Drug Alcohol Depend*. 2019;201:29–37.
83. Kim I-S, et al. Reduced corpus callosum white matter microstructural integrity revealed by diffusion tensor eigenvalues in abstinent methamphetamine addicts. *Neurotoxicology*. 2009;30(2):209–213.
84. Salo R, et al. Cognitive control and white matter callosal microstructure in methamphetamine-dependent subjects: a diffusion tensor imaging study. *Biol Psychiatry*. 2009;65(2):122–128.
85. Suchting R, et al. A meta-analysis of tract-based spatial statistics studies examining white matter integrity in cocaine use disorder. *Addict Biol*. 2021;26(2):e12902.
86. Romero MJ, et al. Cocaine addiction: diffusion tensor imaging study of the inferior frontal and anterior cingulate white matter. *Psychiatry Res*. 2010;181(1):57–63.
87. Moeller FG, et al. Reduced anterior corpus callosum white matter integrity is related to increased impulsivity and reduced discriminability in cocaine-dependent subjects: diffusion tensor imaging. *Neuropsychopharmacology*. 2005;30(3):610–617.
88. Vaquero L, et al. Cocaine addiction is associated with abnormal prefrontal function, increased striatal connectivity and sensitivity to monetary incentives, and decreased connectivity outside the human reward circuit. *Addict Biol*. 2017;22(3):844–856.
89. Xu J, et al. White matter integrity is associated with treatment outcome measures in cocaine dependence. *Neuropsychopharmacology*. 2010;35(7):1541–1549.
90. He Q, et al. White matter integrity alternations associated with cocaine dependence and long-term abstinence: Preliminary findings. *Behav Brain Res*. 2020;379:112388.
91. Sun Y, et al. Disrupted white matter structural connectivity in heroin abusers. *Addict Biol*. 2017;22(1):184–195.
92. Wollman SC, et al. White matter abnormalities in long-term heroin users: a preliminary neuroimaging meta-analysis. *Am J Drug Alcohol Abuse*. 2015;41(2):133–138.
93. Wang Y, et al. White matter impairment in heroin addicts undergoing methadone maintenance treatment and prolonged abstinence: a preliminary DTI study. *Neurosci Lett*. 2011;494(1):49–53.
94. Li W, et al. White matter impairment in chronic heroin dependence: a quantitative DTI study. *Brain Res*. 2013;1531:58–64.
95. Qiu Y, et al. Progressive white matter microstructure damage in male chronic heroin dependent individuals: a DTI and TBSS study. *PLoS One*. 2013;8(5):e63212.
96. Lu L, et al. Potential brain recovery of frontostriatal circuits in heroin users after prolonged abstinence: A preliminary study. *J Psychiatr Res*. 2022;152:326–334.
97. Shen Y, et al. Disrupted integrity of white matter in heroin-addicted subjects at different abstinent time. *J Addict Med*. 2012;6(2):172–176.
98. Ma L, et al. Altered white matter in cocaine-dependent subjects with traumatic brain injury: A diffusion tensor imaging study. *Drug Alcohol Depend*. 2015;151:128–134.
99. Li W, et al. Brain white matter integrity in heroin addicts during methadone maintenance treatment is related to relapse propensity. *Brain Behav*. 2016;6(2):e00436.
100. Eleanor LSC, et al. DNA methylation and protein markers of chronic inflammation and their associations with brain and cognitive aging. *Neurology*.

2021;97(23):e2340–e2352.
101. Brosseron F, et al. Serum IL-6, sAXL, and YKL-40 as systemic correlates of reduced brain structure and function in Alzheimer's disease: results from the DELCODE study. *Alzheimers Res Ther*. 2023;15(1):13.
102. Conole ELS, et al. DNA methylation and protein markers of chronic inflammation and their associations with brain and cognitive aging. *Neurology*. 2021;97(23):e2340–e2352.
103. Zhang H, et al. The relationship between inflammatory markers and voxel-based gray matter volumes in nondemented older adults. *Neurobiol Aging*. 2016;37:138–146.
104. Leclercq S, et al. Role of intestinal permeability and inflammation in the biological and behavioral control of alcohol-dependent subjects. *Brain Behav Immun*. 2012;26(6):911–918.
105. Karoly HC, et al. TLR4 methylation moderates the relationship between alcohol use severity and gray matter loss. *J Stud Alcohol Drugs*. 2017;78(5):696–705.
106. Kohno M, et al. The relationship between interleukin-6 and functional connectivity in methamphetamine users. *Neurosci Lett*. 2018;677:49–54.
107. Wang TY, et al. Correlation of cytokines, BDNF levels, and memory function in patients with opioid use disorder undergoing methadone maintenance treatment. *Drug Alcohol Depend*. 2018;191:6–13.
108. Lu R-B, et al. Correlation between interleukin-6 levels and methadone maintenance therapy outcomes. *Drug Alcohol Depend*. 2019;204:107516.
109. Woodcock EA, et al. Quantification of [^{11}C] PBR28 data after systemic lipopolysaccharide challenge. *EJNMMI Res*. 2020;10(1):19.
110. Esposito G, et al. Imaging neuroinflammation in Alzheimer's disease with radiolabeled arachidonic acid and PET. *J Nucl Med*. 2008;49(9):1414–1421.
111. Doot RK, et al. [^{18}F]NOS PET brain imaging suggests elevated neuroinflammation in idiopathic Parkinson's disease. *Cells*. 2022;11(19):3081.
112. Wetherill RR, et al. Molecular imaging of pulmonary inflammation in users of electronic and combustible cigarettes: A Pilot Study. *J Nucl Med*. 2023;64(5):797–802.
113. Otto M, et al. Apremilast effectively inhibits TNFα-induced vascular inflammation in human endothelial cells. *J Eur Acad Dermatol Venereol*. 2022;36(2):237–246.
114. Li MJ, et al. Ibudilast attenuates peripheral inflammatory effects of methamphetamine in patients with methamphetamine use disorder. *Drug Alcohol Depend*. 2020;206:107776.
115. Grodin EN, et al. Effects of ibudilast on central and peripheral markers of inflammation in alcohol use disorder: A randomized clinical trial. *Addict Biol*. 2022;27(4):e13182.
116. Bell RL, et al. Ibudilast reduces alcohol drinking in multiple animal models of alcohol dependence. *Addict Biol*. 2015;20(1):38–42.
117. Grigsby KB, et al. Preclinical and clinical evidence for suppression of alcohol intake by apremilast. *J Clin Invest*. 2023;133(6):e159103.
118. Grodin EN, et al. Ibudilast, a neuroimmune modulator, reduces heavy drinking and alcohol cue-elicited neural activation: a randomized trial. *Transl Psychiatry*. 2021;11(1):355.
119. Mu L, et al. Ibudilast attenuates cocaine self-administration and prime- and cue-induced reinstatement of cocaine seeking in rats. *Neuropharmacology*. 2021;201:108830.
120. Snider SE, et al. Glial cell modulators attenuate methamphetamine self-administration in therat. *Eur J Pharm*. 2013;701(1):124.
121. Metz VE, et al. Effects of ibudilast on the subjective, reinforcing, and analgesic effects of oxycodone in recently detoxified adults with opioid dependence. *Neuropsychopharmacology*. 2017;42(9):1825–1832.
122. Heinzerling KG, et al. Randomized, placebo-controlled trial of targeting neuroinflammation with ibudilast to treat methamphetamine use disorder. *J Neuroimmune Pharmacol*. 2020;15(2):238–248.
123. Heckman PRA, et al. Phosphodiesterase Inhibition and Regulation of Dopaminergic Frontal and Striatal Functioning: Clinical Implications. *Int J Neuropsychopharmacol*. 2016;19(10):pyw030.
124. Liu X, et al. PDE4 inhibition restores the balance between excitation and inhibition in VTA dopamine neurons disrupted by repeated in vivo cocaine exposure. *Neuropsychopharmacology*. 2017;42(10):1991–1999.
125. Wakabayashi Y, et al. First-in-human evaluation of (18)F-PF-06445974, a PET radioligand that preferentially labels phosphodiesterase-4B. *J Nucl Med*. 2022;63(12):1919–1924.
126. Morley KC, et al. N-acetyl cysteine in the treatment of alcohol use disorder in patients with liver disease: Rationale for further research. *Expert Opin Investig Drugs*. 2018;27(8):667–675.
127. Smaga I, et al. N-acetylcysteine in substance use disorder: a lesson from preclinical and clinical research. *Pharmacol Rep*. 2021;73(5):1205–1219.
128. Morley KC, et al. N acetylcysteine in the treatment of alcohol use disorder: a randomized, double-blind, placebo-controlled trial. *Alcohol Alcohol*. 2023;58(5):553–560.
129. Squeglia LM, et al. The effect of N-acetylcysteine on alcohol use during a cannabis cessation trial. *Drug Alcohol Depend*. 2018;185:17–22.
130. Blüml S. Magnetic Resonance spectroscopy: basics. In: Blüml S, Panigrahy A, eds. *MR Spectroscopy of Pediatric Brain Disorders*. Springer New York; 2013:11–23.
131. O'Neill J, et al. Separate and interactive effects of cocaine and alcohol dependence on brain structures and metabolites: quantitative MRI and proton MR spectroscopic imaging. *Addict Biol*. 2001;6(4):347–361.
132. Schweinsburg BC, et al. Chemical pathology in brain white matter of recently detoxified alcoholics: a 1H magnetic resonance spectroscopy investigation of alcohol-associated frontal lobe injury. *Alcohol Clin Exp Res*. 2001;25(6):924–934.
133. Bendszus M, et al. Sequential MR imaging and proton MR spectroscopy in patients who underwent recent detoxification for chronic alcoholism: correlation with clinical and neuropsychological data. *AJNR Am J Neuroradiol*. 2001;22(10):1926–1932.
134. Parks MH, et al. Longitudinal brain metabolic characterization of chronic alcoholics with proton magnetic resonance spectroscopy. *Alcohol Clin Exp Res*. 2002;26(9):1368–1380.
135. Bloomer CW, et al. Magnetic resonance detects brainstem changes in chronic, active heavy drinkers. *Psychiatry Res*. 2004;132(3):209–218.
136. Durazzo TC, et al. Brain metabolite concentrations and neurocognition during short-term recovery from alcohol dependence: Preliminary evidence of the effects of concurrent chronic cigarette smoking. *Alcohol Clin Exp Res*. 2006;30(3):539–551.
137. Meyerhoff DJ, et al. Effects of heavy drinking, binge drinking, and family history of alcoholism on regional brain metabolites. *Alcohol Clin Exp Res*. 2004;28(4):650–661.
138. Ende G, et al. Monitoring the effects of chronic alcohol consumption and abstinence on brain metabolism: a longitudinal proton magnetic resonance spectroscopy study. *Biol Psychiatry*. 2005;58(12):974–980.
139. Mason GF, et al. Cortical gamma-aminobutyric acid levels and the recovery from ethanol dependence: preliminary evidence of modification by cigarette smoking. *Biol Psychiatry*. 2006;59(1):85–93.
140. Lee E, et al. Alteration of brain metabolites in young alcoholics without structural changes. *NeuroReport*. 2007;18(14):1511–1514.
141. Thoma R, et al. Perturbation of the glutamate-glutamine system in alcohol dependence and remission. *Neuropsychopharmacology*. 2011;36(7):1359–1365.
142. Modi S, et al. Brain metabolite changes in alcoholism: localized proton magnetic resonance spectroscopy study of the occipital lobe. *Eur J Radiol*. 2011;79(1):96–100.
143. Mon A, et al. Glutamate, GABA, and other cortical metabolite concentrations during early abstinence from alcohol and their associations with neurocognitive changes. *Drug Alcohol Depend*. 2012;125(1-2):27–36.
144. Hermann D, et al. Translational magnetic resonance spectroscopy reveals excessive central glutamate levels during alcohol withdrawal in humans and rats. *Biol Psychiatry*. 2012;71(11):1015–1021.
145. Xia Y, et al. Effect of metabotropic glutamate receptor 3 genotype on N-acetylaspartate levels and neurocognition in non-smoking, active alcoholics. *Behav Brain Funct*. 2012;8(1):42.
146. Yeo RA, et al. Neurometabolite concentration and clinical features of chronic alcohol use: a proton magnetic resonance spectroscopy study. *Psychiatry Res*. 2013;211(2):141–147.
147. Ende G, et al. Loss of control of alcohol use and severity of alcohol dependence in non-treatment-seeking heavy drinkers are related to lower glutamate in frontal white matter. *Alcohol Clin Exp Res*. 2013;37(10):1643–1649.
148. Abé C, et al. Polysubstance and alcohol dependence: unique abnormalities of magnetic resonance-derived brain metabolite levels. *Drug Alcohol Depend*. 2013;130(1-3):30–37.
149. Bauer J, et al. Craving in alcohol-dependent patients after detoxification is related to glutamatergic dysfunction in the nucleus accumbens and the anterior cingulate cortex. *Neuropsychopharmacology*. 2013;38(8):1401–1408.
150. Silveri MM, et al. Altered anterior cingulate

neurochemistry in emerging adult binge drinkers with a history of alcohol-induced blackouts. *Alcohol Clin Exp Res*. 2014;38(4):969–979.
151. Bagga D, et al. Impaired visual information processing in alcohol-dependent subjects: a proton magnetic resonance spectroscopy study of the primary visual cortex. *J Stud Alcohol Drugs*. 2014;75(5):817–826.
152. de Souza RSM, et al. Lower choline rate in the left prefrontal cortex is associated with higher amount of alcohol use in alcohol use disorder. *Front Psychiatry*. 2018;9:563.
153. Prisciandaro JJ, et al. Brain glutamate, GABA, and glutamine levels and associations with recent drinking in treatment-naïve individuals with alcohol use disorder versus light drinkers. *Alcohol Clin Exp Res*. 2019;43(2):221–226.
154. Grecco GG, et al. Anterior cingulate cortex metabolites and white matter microstructure: a multimodal study of emergent alcohol use disorder. *Brain Imaging Behav*. 2021;15(5):2436–2444.
155. Schulte MHJ, et al. Prefrontal Glx and GABA concentrations and impulsivity in cigarette smokers and smoking polysubstance users. *Drug Alcohol Depend*. 2017;179:117–123.
156. Steinegger CA, et al. Neurometabolic alterations in the nucleus accumbens of smokers assessed with ^{1}H magnetic resonance spectroscopy: The role of glutamate and neuroinflammation. *Addict Biol*. 2021;26(6):e13027.
157. Bagga D, et al. Metabolic dynamics in the prefrontal cortex during a working memory task in young adult smokers. *Eur Addict Res*. 2021;27(6):428–438.
158. Ke Y, et al. Frontal lobe GABA levels in cocaine dependence: a two-dimensional, J-resolved magnetic resonance spectroscopy study. *Psychiatry Res*. 2004;130(3):283–293.
159. Yang S, et al. Lower glutamate levels in rostral anterior cingulate of chronic cocaine users — A 1H-MRS study using TE-averaged PRESS at 3 T with an optimized quantification strategy. *Psychiatry Res*. 2009;174(3):171.
160. Martinez D, et al. Imaging glutamate homeostasis in cocaine addiction with the metabotropic glutamate receptor 5 positron emission tomography radiotracer [(11)C]ABP688 and magnetic resonance spectroscopy. *Biol Psychiatry*. 2014;75(2):165–171.
161. Hulka LM, et al. Glutamatergic and neurometabolic alterations in chronic cocaine users measured with (1) H-magnetic resonance spectroscopy. *Addict Biol*. 2016;21(1):205–217.
162. Crocker CE, et al. Enduring changes in brain metabolites and executive functioning in abstinent cocaine users. *Drug Alcohol Depend*. 2017;178:435–442.
163. Ernst T, et al. Evidence for long-term neurotoxicity associated with methamphetamine abuse: A 1H MRS study. *Neurology*. 2000;54(6):1344–1349.
164. Nordahl TE, et al. Low N-acetyl-aspartate and high choline in the anterior cingulum of recently abstinent methamphetamine-dependent subjects: a preliminary proton MRS study. Magnetic resonance spectroscopy. *Psychiatry Res*. 2002;116(1-2):43–52.
165. Chang L, et al. Additive effects of HIV and chronic methamphetamine use on brain metabolite abnormalities. *Am J Psychiatry*. 2005;162(2):361–369.
166. Sung YH, et al. Relationship between N-acetyl-aspartate in gray and white matter of abstinent methamphetamine abusers and their history of drug abuse: a proton magnetic resonance spectroscopy study. *Drug Alcohol Depend*. 2007;88(1):28–35.
167. Salo R, et al. Spatial inhibition and the visual cortex: a magnetic resonance spectroscopy imaging study. *Neuropsychologia*. 2011;49(5):830–838.
168. Sung YH, et al. Decreased frontal N-acetylaspartate levels in adolescents concurrently using both methamphetamine and marijuana. *Behav Brain Res*. 2013;246:154–161.
169. Howells FM, et al. 1H-magnetic resonance spectroscopy (1H-MRS) in methamphetamine dependence and methamphetamine induced psychosis. *Schizophrenia Research*. 2014;153(1):122.
170. Crocker CE, et al. Prefrontal glutamate levels differentiate early phase schizophrenia and methamphetamine addiction: a (1)H MRS study at 3Tesla. *Schizophr Res*. 2014;157(1-3):231–237.
171. Lin JC, et al. Investigating the microstructural and neurochemical environment within the basal ganglia of current methamphetamine abusers. *Drug Alcohol Depend*. 2015;149:122–127.
172. Su H, et al. Decreased GABA concentrations in left prefrontal cortex of methamphetamine dependent patients: A proton magnetic resonance spectroscopy study. *J Clin Neurosci*. 2020;71:15–20.
173. Liu XL, et al. Quantifying absolute glutamate concentrations in nucleus accumbens of prescription opioid addicts by using ^{1}H MRS. *Brain Behav*. 2017;7(8):e00769.
174. Chang L, et al. Combined and independent effects of chronic marijuana use and HIV on brain metabolites. *J Neuroimmune Pharmacol*. 2006;1(1):65–76.
175. Silveri MM, et al. Preliminary evidence for white matter metabolite differences in marijuana-dependent young men using 2D J-resolved magnetic resonance spectroscopic imaging at 4 Tesla. *Psychiatry Res*. 2011;191(3):201–211.
176. Pfefferbaum A, Sullivan EV. Microstructural but not macrostructural disruption of white matter in women with chronic alcoholism. *Neuroimage*. 2002;15(3):708–718.
177. Pfefferbaum A, et al. Dysmorphology and microstructural degradation of the corpus callosum: Interaction of age and alcoholism. *Neurobiol Aging*. 2006;27(7):994–1009.
178. Pfefferbaum A, et al. Supratentorial profile of white matter microstructural integrity in recovering alcoholic men and women. *Biol Psychiatry*. 2006;59(4):364–372.
179. De Bellis MD, et al. Diffusion tensor measures of the corpus callosum in adolescents with adolescent onset alcohol use disorders. *Alcohol Clin Exp Res*. 2008;32(3):395–404.
180. Chanraud S, et al. Diffusion tensor tractography in mesencephalic bundles: relation to mental flexibility in detoxified alcohol-dependent subjects. *Neuropsychopharmacology*. 2009;34(5):1223–1232.
181. Yeh P-H, et al. Tract-Based Spatial Statistics (TBSS) of diffusion tensor imaging data in alcohol dependence: abnormalities of the motivational neurocircuitry. *Psychiatry Res*. 2009;173(1):22–30.
182. Konrad A, et al. Broad disruption of brain white matter microstructure and relationship with neuropsychological performance in male patients with severe alcohol dependence. *Alcohol Alcohol*. 2012;47(2):118–126.
183. Zorlu N, et al. Abnormal white matter integrity and decision-making deficits in alcohol dependence. *Psychiatry Res*. 2013;214(3):382–388.
184. Bagga D, et al. Decreased white matter integrity in fronto-occipital fasciculus bundles: relation to visual information processing in alcohol-dependent subjects. *Alcohol*. 2014;48(1):43–53.
185. Zorlu N, et al. Abnormal white matter integrity in long-term abstinent alcohol dependent patients. *Psychiatry Res*. 2014;224(1):42–48.
186. Chumin EJ, et al. Differences in white matter microstructure and connectivity in nontreatment-seeking individuals with alcohol use disorder. *Alcohol Clin Exp Res*. 2018;42(5):889–896.
187. Sawyer KS, et al. Cerebral white matter sex dimorphism in alcoholism: a diffusion tensor imaging study. *Neuropsychopharmacology*. 2018;43(9):1876–1883.
188. Pandey AK, et al. Lower prefrontal and hippocampal volume and diffusion tensor imaging differences reflect structural and functional abnormalities in abstinent individuals with alcohol use disorder. *Alcohol Clin Exp Res*. 2018;42(10):1883–1896.
189. Wiers CE, et al. Elevated thalamic glutamate levels and reduced water diffusivity in alcohol use disorder: Association with impulsivity. *Psychiatry Res Neuroimaging*. 2020;305:111185.
190. Bracht T, et al. The role of the orbitofrontal cortex and the nucleus accumbens for craving in alcohol use disorder. *Transl Psychiatry*. 2021;11(1):267.
191. Lee J, et al. White matter integrity in alcohol-dependent patients with long-term abstinence. *Medicine (Baltimore)*. 2021;100(21):e26078.
192. Kisner MA, et al. Evaluating effects of sex and age on white matter microstructural alterations in alcohol use disorder: A diffusion tensor imaging study. *Alcohol Clin Exp Res*. 2021;45(9):1790–1803.
193. Yoder KK, et al. Effects of acute alcohol exposure and chronic alcohol use on neurite orientation dispersion and density imaging (NODDI) parameters. *Psychopharmacology (Berl)*. 2023;240(7):1465–1472.
194. Wu F, et al. The disruption of white matter integrity of systemic striatal circuits in alcohol-dependent males with physiological cue reactivity. *Addict Biol*. 2023;28(4):e13273.
195. Paul RH, et al. Chronic cigarette smoking and the microstructural integrity of white matter in healthy adults: a diffusion tensor imaging study. *Nicotine Tob Res*. 2008;10(1):137–147.
196. Zhang X, et al. Factors underlying prefrontal and insula structural alterations in smokers. *Neuroimage*. 2011;54(1):42–48.
197. Liao Y, et al. Bilateral fronto-parietal integrity in young chronic cigarette smokers: a diffusion tensor imaging study. *PLoS One*. 2011;6(11):e26460.
198. Lin F, et al. Heavy smokers show abnormal microstructural integrity in the anterior corpus callosum: a diffusion tensor imaging study with tract-based spatial statistics. *Drug Alcohol Depend*.

2013;129(1–2):82–87.
199. Umene-Nakano W, et al. Abnormal white matter integrity in the corpus callosum among smokers: tract-based spatial statistics. *PLoS One*. 2014;9(2):e87890.
200. Savjani RR, et al. Characterizing white matter changes in cigarette smokers via diffusion tensor imaging. *Drug Alcohol Depend*. 2014;145:134–142.
201. Yu D, et al. White matter integrity in young smokers: a tract-based spatial statistics study. *Addict Biol*. 2016;21(3):679–687.
202. Li Y, et al. The implication of salience network abnormalities in young male adult smokers. *Brain Imaging Behav*. 2017;11(4):943–953.
203. Wang S, et al. Abnormal white matter microstructure among early adulthood smokers: a tract-based spatial statistics study. *Neurol Res*. 2017;39(12):1094–1102.
204. Bi Y, et al. White matter integrity of central executive network correlates with enhanced brain reactivity to smoking cues. *Hum Brain Mapp*. 2017;38(12):6239–6249.
205. Yuan K, et al. Abnormal frontostriatal tracts in young male tobacco smokers. *Neuroimage*. 2018;183:346–355.
206. Bagga D, et al. Investigating sex-specific characteristics of nicotine addiction using metabolic and structural magnetic resonance imaging. *Eur Addict Res*. 2018;24(6):267–277.
207. Kangiser MM, et al. Nicotine effects on white matter microstructure in young adults. *Arch Clin Neuropsychol*. 2020;35(1):10–21.
208. Huang H, et al. Evaluating the changes of white matter microstructures in tobacco addicts based on diffusion tensor imaging. *Med Sci Monit*. 2020;26:e919105.
209. Wang C, et al. Abnormal white matter tracts of insula in smokers. *Brain Imaging Behav*. 2021;15(4):1955–1965.
210. Zhou M, et al. Right arcuate fasciculus and left uncinate fasciculus abnormalities in young smoker. *Addict Biol*. 2022;27(2):e13132.
211. Lim KO, et al. Reduced frontal white matter integrity in cocaine dependence: a controlled diffusion tensor imaging study. *Biol Psychiatry*. 2002;51(11):890–895.
212. Lim KO, et al. Brain macrostructural and microstructural abnormalities in cocaine dependence. *Drug Alcohol Depend*. 2008;92(1-3):164–172.
213. Ma L, et al. Diffusion tensor imaging in cocaine dependence: regional effects of cocaine on corpus callosum and effect of cocaine administration route. *Drug Alcohol Depend*. 2009;104(3):262–267.
214. Lane SD, et al. Diffusion tensor imaging and decision making in cocaine dependence. *PLoS One*. 2010;5(7):e11591.
215. Bell RP, et al. Assessing white matter integrity as a function of abstinence duration in former cocaine-dependent individuals. *Drug Alcohol Depend*. 2011;114(2-3):159–168.
216. Ma L, et al. A preliminary longitudinal study of white matter alteration in cocaine use disorder subjects. *Drug Alcohol Depend*. 2017;173:39–46.
217. Tondo LP, et al. White matter deficits in cocaine use disorder: convergent evidence from in vivo diffusion tensor imaging and ex vivo proteomic analysis. *Transl Psychiatry*. 2021;11(1):252.
218. Meade CS, et al. Brain multimodal co-alterations related to delay discounting: a multimodal MRI fusion analysis in persons with and without cocaine use disorder. *BMC Neurosci*. 2021;22(1):51.
219. Ottino-González J, et al. White matter microstructure differences in individuals with dependence on cocaine, methamphetamine, and nicotine: Findings from the ENIGMA-Addiction working group. *Drug Alcohol Depend*. 2022;230:109185.
220. Gaudreault P-O, et al. Whole-brain white matter abnormalities in human cocaine and heroin use disorders: association with craving, recency, and cumulative use. *Mol Psychiatry*. 2023;28(2):780–791.
221. Hodges CB, et al. Chronic cocaine use and white matter coherence: a diffusion tensor imaging study. *J Stud Alcohol Drugs*. 2023;84(4):585–597.
222. Chung A, et al. Decreased frontal white-matter integrity in abstinent methamphetamine abusers. *Int J Neuropsychopharmacol*. 2007;10(6):765–775.
223. Alicata D, et al. Higher diffusion in striatum and lower fractional anisotropy in white matter of methamphetamine users. *Psychiatry Res*. 2009;174(1):1–8.
224. Tobias MC, et al. White-matter abnormalities in brain during early abstinence from methamphetamine abuse. *Psychopharmacology (Berl)*. 2010;209(1):13–24.
225. Daumann J, et al. Medial prefrontal gray matter volume reductions in users of amphetamine-type stimulants revealed by combined tract-based spatial statistics and voxel-based morphometry. *Neuroimage*. 2011;54(2):794–801.
226. Lederer K, et al. Frontal white matter changes and aggression in methamphetamine dependence. *Metab Brain Dis*. 2016;31(1):53–62.
227. Uhlmann A, et al. White matter microstructure and impulsivity in methamphetamine dependence with and without a history of psychosis. *Hum Brain Mapp*. 2016;37(6):2055–2067.
228. Andres T, et al. Brain Microstructure and Impulsivity Differ between Current and Past Methamphetamine Users. *J Neuroimmune Pharmacol*. 2016;11(3):531–541.
229. Li Y, et al. Microstructures in striato-thalamo-orbitofrontal circuit in methamphetamine users. *Acta Radiol*. 2017;58(11):1378–1385.
230. Li Y, et al. Lower fractional anisotropy in the gray matter of amygdala-hippocampus-nucleus accumbens circuit in methamphetamine users: an in vivo diffusion tensor imaging study. *Neurotox Res*. 2018;33(4):801–811.
231. Zhou Y, et al. Association between white matter microstructure and cognitive function in patients with methamphetamine use disorder. *Hum Brain Mapp*. 2023;44(2):304–314.
232. Liu H, et al. Disrupted white matter integrity in heroin dependence: a controlled study utilizing diffusion tensor imaging. *Am J Drug Alcohol Abuse*. 2008;34(5):562–575.
233. Bora E, et al. White matter microstructure in opiate addiction. *Addict Biol*. 2012;17(1):141–148.
234. Wang X, et al. Reversible brain white matter microstructure changes in heroin addicts: a longitudinal study. *Addict Biol*. 2013;18(4):727–728.
235. Ma X, et al. Aberrant default-mode functional and structural connectivity in heroin-dependent individuals. *PLoS One*. 2015;10(4):e0120861.
236. Lu L, et al. Brain recovery of the NAc fibers and prediction of craving changes in person with heroin addiction: A longitudinal study. *Drug Alcohol Depend*. 2023;243:109749.